Vol. 632: 81–100, 2019
https://doi.org/10.3354/meps13151

MARINE ECOLOGY PROGRESS SERIES
Mar Ecol Prog Ser

Published December 12

Duality of trophic supply and hydrodynamic connectivity drives spatial patterns of Pacific oyster recruitment

Franck Lagarde[1,2,*], Annie Fiandrino[1], Martin Ubertini[3], Emmanuelle Roque d'Orbcastel[1], Serge Mortreux[1], Claude Chiantella[1], Béatrice Bec[4], Delphine Bonnet[4], Cécile Roques[4], Ismaël Bernard[5], Marion Richard[1], Thomas Guyondet[6], Stéphane Pouvreau [7], Christophe Lett[1]

[1]MARBEC, Univ. Montpellier, CNRS, IRD, Ifremer, 34200 Sète, France
[2]Sorbonne Université, Collège Doctoral, 75005 Paris, France
[3]POS3IDON S.A.S, 35400 Saint-Malo, France
[4]MARBEC, Univ. Montpellier, CNRS, IRD, Ifremer, 34095 Montpellier, France
[5]Eurêka Mer S.A.S, 22740 Lézardrieux, France
[6]Ministère Pêche et Océans, Moncton, NB E1C 5K4, Canada
[7]LEMAR, Ifremer, CNRS, IRD, UBO, 29280 Plouzané, France

ABSTRACT: The recent discovery of Pacific oyster *Crassostrea gigas* (also known as *Magallana gigas*) spatfields in a Mediterranean lagoon intensely exploited for shellfish farming (Thau lagoon) revealed significant contrasts in spatial patterns of recruitment. We evaluated the processes that drive spatial patterns in oyster recruitment by comparing observed recruitment, simulated hydrodynamic connectivity and ecological variables. We hypothesized that spatial variability of recruitment depends on (1) hydrodynamic connectivity and (2) the ecology of the larval supply, settlement, metamorphosis, survival and biotic environmental parameters. We assessed recruitment at 6–8 experimental sites by larval sampling and spat collection inside and outside oyster farming areas and on an east–west gradient, from 2012–2014. Hydrodynamic connectivity was simulated using a numerical 3D transport model assessed with a Eulerian indicator. The supply of large umbo larvae did not differ significantly inside and outside oyster farming areas, whereas the supply of pediveligers to sites outside shellfish farms was structured by hydrodynamic connectivity. Inside shellfish farming zones, unfavorable conditions due to trophic competition with filter-feeders jeopardized their settlement. In this case, our results suggest loss of settlement competence by oyster larvae. This confirms our hypothesis of top-down trophic control by the oysters inside farming zones of Thau lagoon in summer that fails to meet the ecological requirements of these areas as oyster nurseries. Knowledge of oyster dispersal, connectivity and recruitment in coastal lagoons will help local development of sustainable natural spat collection. On a global scale, our method could be transposed to other basins or used for other species such as mussels, clams or scallops, to better understand the spatial patterns of bivalve recruitment. Management of the oyster industry based on natural spat collection will help develop a sustainable activity, based on locally adapted oyster strains but also by reducing the risks of transferring pathogens between basins and the global carbon footprint of this industry.

KEY WORDS: *Crassostrea gigas* · Coastal lagoon · Larval ecology · Spatial patterns · Connectivity · Settlement · Recruitment · Oligotrophication

*Corresponding author: franck.lagarde@ifremer.fr

1. INTRODUCTION

More knowledge on reproduction and recruitment is needed to improve our understanding of marine population dynamics and for fishery stock management, both of which face changing conditions ranging from local anthropogenic pressures to global climate change (Hunt & Scheibling 1997a, Cowen et al. 2007, Pérez-Ruzafa et al. 2019). The early life of most marine benthic invertebrates includes spawning, larval development, dispersal (Todd 1998, Cowen & Sponaugle 2009), settlement (Gaines et al. 1985) and ultimately recruitment of juveniles into the host ecosystem (Keough & Downes 1982). These different processes are incorporated in the concept of marine population connectivity between spawning and recruitment areas (Pineda et al. 2007). Marine connectivity is defined by the rate of transfer of organisms between locations (Bryan-Brown et al. 2017). Numerical models are widely used to assess hydrodynamic connectivity in order to compare different release zones (Solidoro et al. 2004, Fiandrino et al. 2017), identify dispersal pathways and quantify cumulated fluxes of tracers per volume or area (Ghezzo et al. 2015, Lagarde et al. 2015, Thomas et al. 2016). These models are also used to highlight physical versus biological and ecological functioning at different spatial and temporal scales. The number of studies conducted to improve our knowledge of connectivity has increased markedly over the last 30 yr (Elsäßer et al. 2013, Bryan-Brown et al. 2017). Recently, connectivity studies that combine simulation modeling and field work with direct observations of larval development have been conducted (Smyth et al. 2016). However, Ghezzo et al. (2015) drew attention to the lack of connectivity studies combining modeling and field work that include direct data on larval development and environmental factors. The aim of the present study was to fill this knowledge gap by studying the transition from pelagic to benthic life of the Pacific oyster *Crassostrea gigas* (also known as *Magallana gigas*) in a coastal, nanotidal semi-enclosed Mediterranean lagoon.

In most marine larvae, the transition between pelagic and benthic development is induced by settlement and metamorphosis competences that insure successful recruitment (Coon et al. 1990). Settlement is initially driven by the hydrodynamics of the ecosystem (Todd 1998, Wing et al. 2003), but the biological properties of the organisms also play an important role in the physiological (trophic diet, food limitation or energy depletion), ethological (migration, trophic settlement trigger) and ecological (predation, competition) aspects of the development phase (Hunt & Scheibling 1997a).

Despite the economic importance of Pacific oysters *C. gigas*, there are still gaps in our knowledge of their *in situ* life, including early benthic settlement and post-settlement stages (Bayne 2017, Lagarde et al. 2018). The origins of recruitment variability are still not completely known because of species and habitat specificities and the complexity of ecosystem dynamics that prevent generalization (Roughgarden et al. 1988). Such complexity is best explained by studying the general functioning of recruitment and production of each species at local scale (Hori et al. 2018).

In a recent study, we reported that the discovery of Pacific oyster spatfields in the Mediterranean Thau lagoon highlighted the influence of strong temporal, biological and ecological processes on recruitment (Lagarde et al. 2017). These results suggest that, in the Thau lagoon, time windows for oyster recruitment depend on autotroph vs. heterotroph species domination related to water temperature and oxygen conditions. Such results are best obtained by examining several larval stages, to determine the relative importance of each stage and any potential ecological problems in larval development (Hunt & Scheibling 1997b, Ghezzo et al. 2015, Pouvreau et al. 2018). In addition to the temporal component, spatial patterns in settlement or early post-settlement are known to influence the distribution and abundance of benthic marine invertebrate juveniles and adults (Hunt & Scheibling 1997a, Thomas et al. 2016).

In the present study, the spatial variability of oyster recruitment was investigated using a connectivity approach, and more broadly considering further oyster trophic limitations (i.e. nanophytoplankton and microphytoplankton) due to oligotrophication of Thau lagoon (Collos et al. 2009). Oligotrophication results from a decrease in nutrient inputs due to society's demand for environmental recovery (Collos et al. 2009, Hori et al. 2018). Our specific aim was to explain the spatial pattern of recruitment of *C. gigas* with data produced by both field observations and hydrodynamic modeling in order to establish relationships between larval supply, connectivity and ecological functioning. To this end, we tested the hypothesis that the spatial variability of recruitment depends on hydrodynamic connectivity and on larval ecology at settlement and recruitment on immersed collectors (Collos et al. 2009, Souchu et al. 2010, Lagarde et al. 2017). Our overall objective was to disentangle and evaluate the comparative roles of connectivity and biotic factors. Understanding the population connectivity of oysters should result in societal gain by informing the devel-

opment of sustainable natural spatfall collection practices. On a more global scale, the added value of this work will be in improving the management of areas intensely exploited by mollusk farming, where oligotrophication and sustainable exploitation have to be adjusted to insure continuing ecological functions (such as a mollusk nursery) and the ecosystem services they provide, such as oyster spat collection.

2. MATERIALS AND METHODS

2.1. Study site

Our study site was located in the French Thau lagoon, on the northern coast of the Mediterranean Sea in the Gulf of Lion (Fig. 1). This restricted nanotidal semi-enclosed hydrosystem (Kjerfve 1994) covers an area of 7500 ha (19 × 4.5 km) on a northeast–southwest axis and has a mean depth of 4 m (Fiandrino et al. 2017). The lagoon is influenced by seawater inputs from the Mediterranean Sea that enter through 2 artificial inlets: the Sète channel in the north, which accounts for 90% of seawater exchanges, and the Pisse-Saumes channel in the south. Wild oyster stocks are negligible compared to oyster farming. Twenty percent of the total Thau lagoon area is dedicated to intense cultivation of mussels and oysters; other areas are devoid of shellfish farming and are used for fishing.

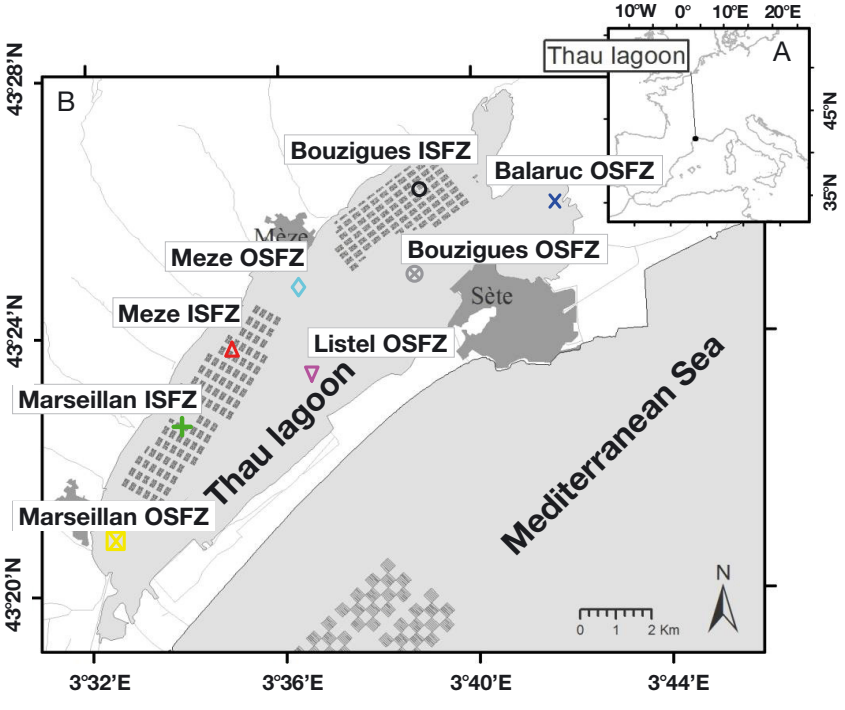

Fig. 1. (A) Thau lagoon bordering the Mediterranean Sea in the South of France and (B) Pacific oyster sampling sites in Thau lagoon. ISFZ: inside the shellfish farming zone (monitoring took place under farm structures); OSFZ: outside the shellfish farming zone (monitoring took place at specially designed mooring systems; see Lagarde et al. 2017). Colored symbols identify 3 ISFZ sites (Marseillan_ISFZ, Meze_ISFZ and Bouzigues_ISFZ) and 5 OSFZ sites (Marseillan_OSFZ, Listel_OSFZ, Meze_OSFZ, Bouzigues_OSFZ and Balaruc_OSFZ) where pelagic larvae and benthic Pacific oyster larvae, spat abundances, hydrological and plankton data were monitored. Grey boxes: shellfish farms; dark grey areas: towns

2.2. Larval and recruitment abundance

A total of 8 spatfall sites in Thau lagoon (Fig. 1) were monitored to assess pre-settled oyster larvae and post-settled spat abundances in pelagic and benthic compartments: 3 sites were located inside the shellfish farming zones (hereafter ISFZ: Marseillan_ISFZ, Meze_ISFZ and Bouzigues_ISFZ) and 5 outside (OSFZ: Marseillan_OSFZ, Listel_OSFZ, Meze_OSFZ, Bouzigues_OSFZ and Balaruc_OSFZ).

Pelagic and benthic larval abundances of *Crassostrea gigas* were assessed in the years 2012, 2013 and 2014 from June to September, which corresponds to the reproductive window of Pacific oysters in Thau lagoon (Fig. 2). Pelagic larvae were quantified twice a week using a standard protocol provided by the French Oyster Larvae Monitoring Network (French acronym VELYGER) (Pouvreau et al. 2013, 2016). A sampling volume of 1.5 m^3 was pumped and filtered through a 40 µm plankton net to count oyster larvae, ranging on average from D-shaped larvae (60–105 µm), small and medium umbo larvae (106–235 µm) to large umbo larvae (235–400 µm) (Pouvreau 2016). Benthic oyster abundances were estimated on plate collectors (coupelles) every 2 wk at 3 different settler stages: pre-settled larvae as pediveligers (size range: 190–300 µm), young post-larvae after metamorphosis (300–1000 µm) (Coon et al. 1990, Pechenik 2006) and newly settled spat (1–8 mm) (Arakawa 1990).

In the present work, larval development was studied based on 4 different development stages (D-larvae, large umbo larvae, pediveliger and oyster spat). Settlement is defined here as a process of becoming familiar with the substrate through the onset of a behav-

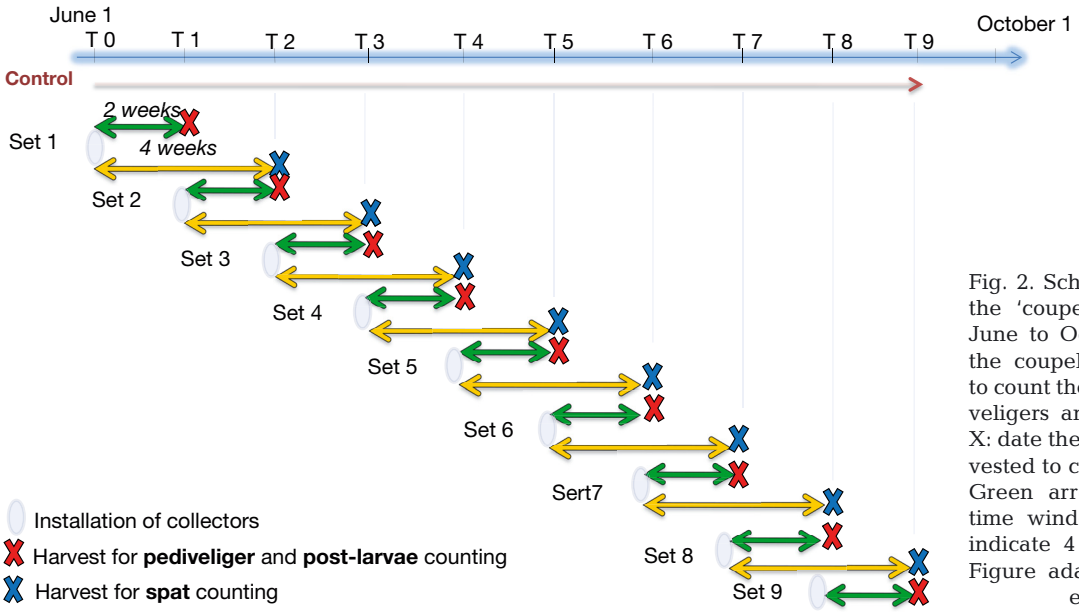

Fig. 2. Schedule for setting up the 'coupelle' collectors from June to October. Red X: date the coupelles were harvested to count the Pacific oyster pediveligers and post-larvae; blue X: date the coupelles were harvested to count the oyster spat. Green arrows indicate 2 wk time windows; yellow arrows indicate 4 wk time windows. Figure adapted from Lagarde et al. (2019)

ioral search for a suitable location, ending with cementation (Pawlik 1992, Rodríguez et al. 1993, Pineda et al. 2009). Metamorphosis is the next stage before recruitment (Coon et al. 1990, Fitt et al. 1990). Recruitment is confirmed when oyster juveniles reach 1–8 mm in size (Lagarde et al. 2017) and can be seen with the naked eye by observers after the collectors have been immersed for 4 wk (Booth & Brosnan 1995).

To enable collection of these benthic stages, the sites were equipped with 2 series of 3 replicate collectors (Figs. 3–5). One set was submersed for 2 wk to collect pediveligers; the second set was submersed for 4 wk to collect oyster spat (Fig. 2). Each collector was replaced after 4 wk of submersion, meaning that at each sampling site, one series of collectors was replaced every 2 wk throughout the summer.

2.3. Environmental measurements

Environmental parameters (hydrological and plankton samples) were recorded at weekly intervals from June–September in 2012, 2013 and 2014 close to the spatfall sites Listel_OSFZ, Bouzigues_ISFZ and Marseillan_ISFZ. Temperature and salinity were measured twice a week using WTW® probes positioned

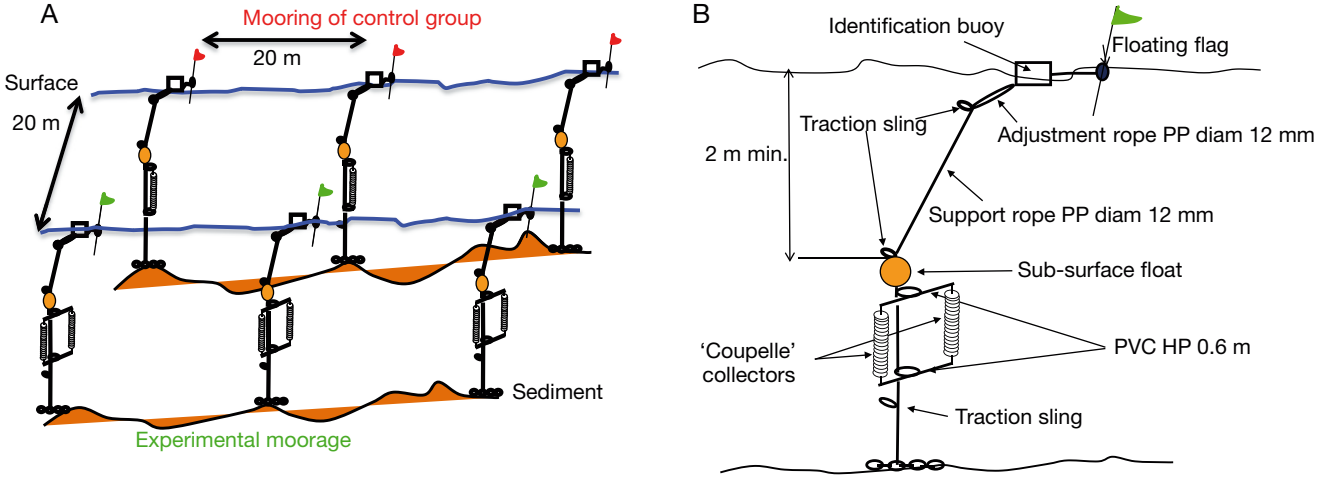

Fig. 3. (A) Sampling site to collect Pacific oyster spat outside the shellfish farming zone with 3 control moorings and 3 replicated spat collection mooring systems. (B) Each mooring system supported a set of 2 'coupelle' collectors. PP: polypropylene; PVC HP: PVC high pressure. The first collector was immersed for 2 wk and the second for 4 wk before being replaced by a new collector for the next series. Figure adapted from Lagarde et al. (2017, 2019)

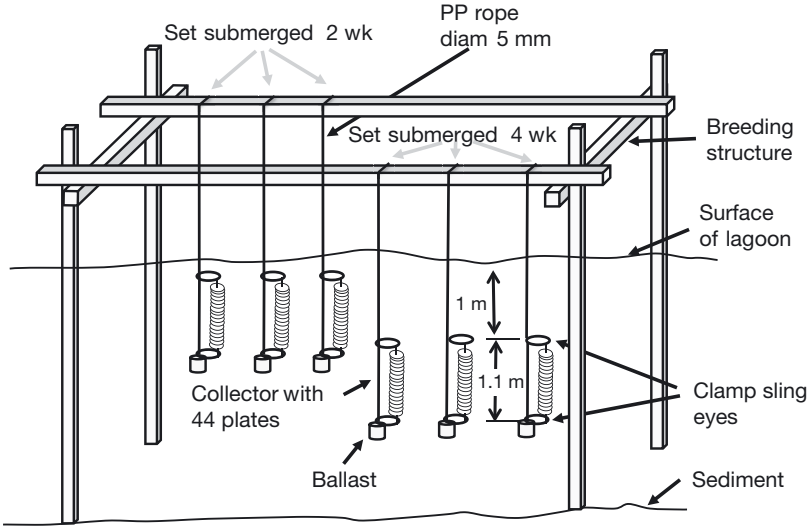

Fig. 4. Mooring system inside the shellfish farming zone. PP: polypropylene. The breeding structure carried a first series of 3 replicate collectors for 2 wk of submersion to assess Pacific oyster pediveliger abundance and a second series of 4 wk of submersion to assess oyster spat. The control set of 3 collectors is not shown

between 1 and 1.5 m below the surface, and averaged weekly.

The biomass and abundance (Table 1) of the planktonic community — bacteria (<1 µm), pico- (<3 µm), nano- (3–20 µm) and microphytoplankton (>20 µm), protozooplankton and mesozooplankton — were monitored at weekly intervals from June–September in 2012, 2013 and 2014 close to spatfall sites Listel_OSFZ, Bouzigues_ISFZ and Marseillan_ISFZ (but not at Listel_OSFZ in 2012) (Lagarde et al. 2017, REPHY 2017). Abundance of potential predators and trophic competitors of *C. gigas* larvae were estimated by taxonomic identification using a binocular microscope (Rose 1933). The trophic competitors group was determined as the sum of copepod nauplii, annelids, barnacles, ascidia and gastropod larvae. Potential predators were assessed as the sum of cladocerans (*Penilia avirostris*, *Podon* spp., and *Evadne* spp.), decapod larvae, mysids and hydrozoa (*Obelia* spp.).

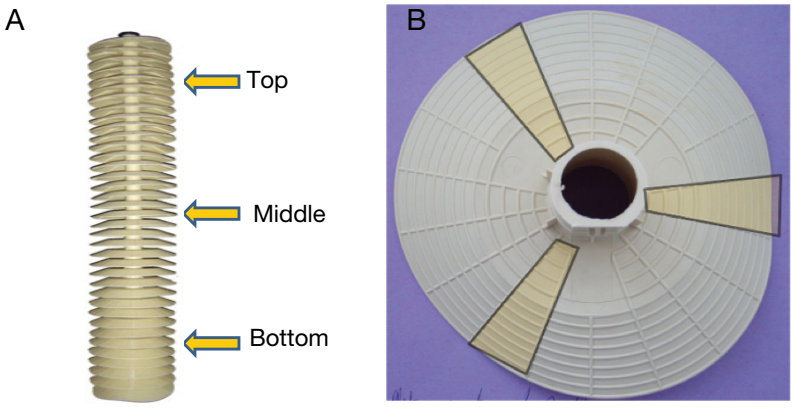

Fig. 5. (A) Pacific oyster sampling strategy at 3 levels (top, middle, bottom) of 'coupelle' collectors (B) top view of 'coupelle' collector with 3 replicated counting subunits in yellow. Figure adapted from Lagarde et al. (2017)

2.4. Hydrodynamic connectivity index

We used an Eulerian approach to study the hydrodynamic processes (Pineda & Reyns 2018). We define hydrodynamic connectivity (Ghezzo et al. 2015) between a finite tracer emission volume of a shellfish zone (V_E) and a finite destination volume (V_D) as the amount of a passive dissolved conservative tracer released from V_E and entering V_D over a given period of time (ΔT). The intrinsic movement of larvae (horizontal swimming and vertical migration) and their mortality were not considered because the focus of the present study was only on the hydrodynamic aspect of connectivity.

To assess hydrodynamic connectivity, we used the 3-dimensional hydrodynamic Model for Application at Regional Scale (MARS-3D; Lazure & Dumas 2008). The MARS-3D model has already been used to simulate water exchange between Thau lagoon and the Mediterranean Sea and validated (Fiandrino et al. 2017). The model grid has a spatial resolution of 100 m. Bathymetry was taken from the 2010 survey by the 'Cellule de qualité des Eaux Littorales' of the Occitanie/Languedoc-Roussillon Region (Bernard et al. 2013). Ten sigma layers were distributed on the vertical axis to represent the bottom and surface boundary layers.

A passive dissolved conservative tracer was homogeneously released throughout the water column in shellfish farming areas at the beginning of the simulation and used to visualize the circulation of water bodies associated with larval transport. The amount of tracer entering the volume of each cell of the horizontal 2D grid (integrated over the whole water column), $Q_D(i,j,T_{Integ})$, was cumulated over T_{Integ} = 18 d (i and j are mesh indices), corre-

Table 1. Variables characterizing the interactions between the environment and Pacific oyster larvae at the sampling sites Bouzigues_ISFZ, Marseillan_ISFZ and Listel_OSFZ (see Fig. 1 for site names and locations) monitored from June to the end of September 2012, 2013 and 2014 (except Listel_OSFZ in 2012). Each environmental variable was averaged over a 22 d period preceding retrieval of the collectors. Superscript A: abundance; B: biomass; (–) no transformation or no abbreviation

Variables	Description	Units	Transformation	Abbreviation
Target variables				
Oyster spat	Abundance	ind. plate^{-1}	$\log_{10}(x + 1)$ or power Box-Cox (lambda = –0.63)	log_spat or pbc_spat
Pediveligers	Abundance	ind. plate^{-1}	$\log_{10}(x + 1)$	log_pedi
Environmental variables				
Connectivity Index	Daily ratio	% d^{-1}	–	
Max. D-larvae	Max. D-larvae abund.	ind. m^{-3}	$\log_{10}(x + 1)$	log_max_DL
Max. large umbo larvae	Max. large umbo larvae abund.	ind. m^{-3}	$\log_{10}(x + 1)$	log_max_UL
Temperature	Daily average	°C	–	–
Salinity	Daily average	No units	–	–
Bacteria	Abundance	10^6 cells l^{-1}	$\log_{10}(x + 1)$	log_bact^A
Autotrophic picoeukaryotes	Abundance	10^6 cells l^{-1}	$\log_{10}(x + 1)$	log_peuk_tot^A
Picocyanobacteria	Abundance	10^6 cells l^{-1}	$\log_{10}(x + 1)$	log_cyan^A
Picophytoplankton	Abundance	10^6 cells l^{-1}	$\log_{10}(x + 1)$	log_pico_tot^A
Nanophytoplankton	Abundance	10^6 cells l^{-1}	$\log_{10}(x + 1)$	log_nano^A
Cryptophycae	Abundance	10^6 cells l^{-1}	$\log_{10}(x + 1)$	log_crypto^A
Nanophytoplankton + Cryptophycae	Abundance	10^6 cells l^{-1}	$\log_{10}(x + 1)$	log_nano_tot^A
Heterotrophic flagellates	Abundance	Cells l^{-1}	$\log_{10}(x + 1)$	log_HF^A
Naked ciliates	Abundance	Cells l^{-1}	$\log_{10}(x + 1)$	log_ciliates^A
Tintinnidae	Abundance	Cells l^{-1}	$\log_{10}(x + 1)$	log_tinti^A
Diatoms	Abundance	Cells l^{-1}	$\log_{10}(x + 1)$	log_diatom^A
Dinoflagellates	Abundance	Cells l^{-1}	$\log_{10}(x + 1)$	log_dinoflagellates^A
Chaetoceros	Abundance	Cells l^{-1}	$\log_{10}(x + 1)$	log_chaetoceros^A
Total chlorophyll *a*	Biomass	µg chl *a* l^{-1}	$\log_{10}(x + 1)$	log_total_chloa^B
Picophytoplankton	Biomass	µg chl *a* l^{-1}	$\log_{10}(x + 1)$	log_pico^B
Nanophytoplankton	Biomass	µg chl *a* l^{-1}	$\log(x)$	log_nano_3_20^B
Picophytoplankton + nanophytoplankton	Biomass	µg chl *a* l^{-1}	$\log_{10}(x + 1)$	log_nano_low20^B
Microphytoplankton >20 µm	Biomass	µg l^{-1}	$\log_{10}(x + 1)$	log_micro^B
Competitors	Abundance	ind. m^{-3}	square root(x)	sqrt_comp^A
Predators	Abundance	ind. m^{-3}	$\log_{10}(x + 1)$	log_pred^A

sponding to the potential period of larval settlement (Lagarde et al. 2015, Pouvreau et al. 2015). Integration started 4 d after the tracer was released to reflect the minimum pelagic larval duration (T_{PLD}) observed for *C. gigas*.

The local hydrodynamic connectivity index (CI), $CI(i,j,T_{Integ})$, was then defined as the ratio of $Q_D(i,j,T_{Integ})$ to the total amount of tracer released in shellfish farmed areas (Q_E), $Q_E = [C_{PCT}] \times V_E$, where V_E is the combined volume of all shellfish farming areas and $[C_{PCT}]$ is the vertical concentration in all cells of the grid corresponding to shellfish farming areas (n = 566). To compare observed recruitment and simulated hydrodynamic connectivity, CI values were calculated for the date each collector was harvested to estimate the abundance of pediveligers, i.e. every 2 wk from 1 June to 1 October in 2012, 2013 and 2014:

$$CI(i,j,T_{Integ}) = \frac{Q_D(i,j,T_{Integ})}{Q_E} / T_{Integ} \quad (1)$$

2.5. Simulation setup, forcing and open boundary conditions of the MARS-3D model

Several simulations were run to scan the variability of starting conditions and the following chronology between 1 June and 29 September with a 3 d resolution. Hence, the difference between the start of 2 sequential simulations was 3 d. A total of 50 simulations were started throughout this period, and each simulation ended 1 mo later. In each simulation, the passive conservative tracer was released at the beginning of the simulation with a uniform horizontal concentration in each grid cell containing shellfish farms. A preliminary simulation was run to calculate and record the daily hydrodynamic states of the system from 1 April until 1 October in each of the 3 study years. The recorded daily state of the system was used as the initial hydrodynamic conditions for each of the 50 simulations.

This simulation setup assumed that tracer releases were synchronous. The synchronicity hypothesis is

based on our previous observations that efficient spawning events are synchronous (Lagarde et al. 2015). Since [C_{PCT}] is a constant, the total quantities of tracer released per zone only depend on the volume of the zones (Volume Marseillan/Volume Meze/Volume Bouzigues = 1/1.5/4). Thus, the ratio between Q_E Marseillan, Q_E Meze and Q_E Bouzigues is equal to the ratio of the volumes of the zones.

A detailed description of atmospheric forcing and open boundary conditions for Thau lagoon is provided in Fiandrino et al. (2017). Meteorological data were used to describe the state of the atmospheric boundary layer: wind speed at a height of 10 m, and air pressure at sea level. Chronologies of wind speed and direction were measured directly above Thau lagoon at Marseillan_ISFZ station with a Campbell Scientific datalogger (CR1000) and Ultra Sonic Wind Sensor (Windsonic). Wind speed and direction were considered to be spatially homogenous across the lagoon (Fiandrino et al. 2017). These data were acquired at 1 min intervals and were averaged over 10 min to be consistent with open boundary conditions.

At the open boundary, the model was forced by tide gauge data recorded at 10 min intervals in Sète channel (Holgate et al. 2013) with the 2016 database from the Permanent Service for Mean Sea Level (PSMSL). Temperatures and salinity at the open boundary were monitored every 2 wk by the French National Phytoplankton and Phycotoxin Monitoring Network (REPHY 2017) at the Sète-Mer station, located just off the Sète channel inlet.

2.6. Data analysis

Statistical analyses were performed with R v.3.5.0 (R Core Team 2015). The experimental approach was based on correlative and statistical modeling approaches.

An ANOVA was performed to test the effect of year and sampling site on the recruitment of observed spat abundances with Power Box-Cox transformation (lambda = −0.63). Normality and heteroscedasticity of residuals were checked by visual inspection. Oyster spat recruitment was displayed graphically using comparison of means with 95% confidence intervals.

Box and whisker plots were used to distinguish the effect of situation (ISFZ vs. OSFZ) on larval abundance at the 4 different stages of development (D-larvae, large umbo larvae, pediveligers and spat). We tested the hypothesis that larval abundances did not vary according to ISFZ–OSFZ biocoenosis (under $\log_{10}$ transformation) with a parametric ANOVA if prerequisites of normality, homoscedasticity and independence were respected; otherwise, we used a non-parametric Kruskal-Wallis test.

The 50 simulations over the period from 1 June to 29 September were analyzed to establish yearly maps of averaged hydrodynamic connectivity over the 3 study years. The mean hydrodynamic CI was averaged from the 50 values of indicators calculated over periods of 18 d corresponding to the maximum duration of larval settlement.

A simulated connectivity indicator was calculated using the dates on which spat was collected at the 8 experimental sampling sites. The connectivity indicators are presented as box and whiskers plots. An ANOVA model was fitted with additional Tukey contrasts multiple comparisons of means ('multcomp' package) to differentiate the connectivity levels at the different sampling sites.

The relationship between simulated connectivity and the abundances of the different larval stages is illustrated by means and standard error bars on scatterplots in both the *x* and *y* directions associated with linear regression lines. ANCOVA was used to compare the ISFZ vs. OSFZ regression model with respect to the application conditions (independence, linearity and homoscedasticity).

To further investigate the link between larval abundance and the plankton environment, we used a linear multiple regression with transformed data. The adjusted R^2 was maximized without minimizing collinearity.

3. RESULTS

3.1. Spatial variability of oyster spat recruitment and larvae abundances

We found significant differences in oyster spat recruitment in accordance with the interaction between year and situation (i.e. inside or outside the shellfish farmed zone: situation × year; $p < 0.05$) in Thau lagoon (Fig. 6, Table 2). In 2012, the first significant spat collection was recorded on 13 August, with 126 and 47 spat ind. plate^{-1} at Listel_OSFZ and Bouzigues_ISFZ, respectively (Fig. 6; 2012). The second significant spat harvest took place on 24 September at the same sites but was characterized by lower abundances (45 and 21 ind. plate^{-1} at Bouzigues_ISFZ and Listel_OSFZ, respectively). We also collected 34 ind. plate^{-1}

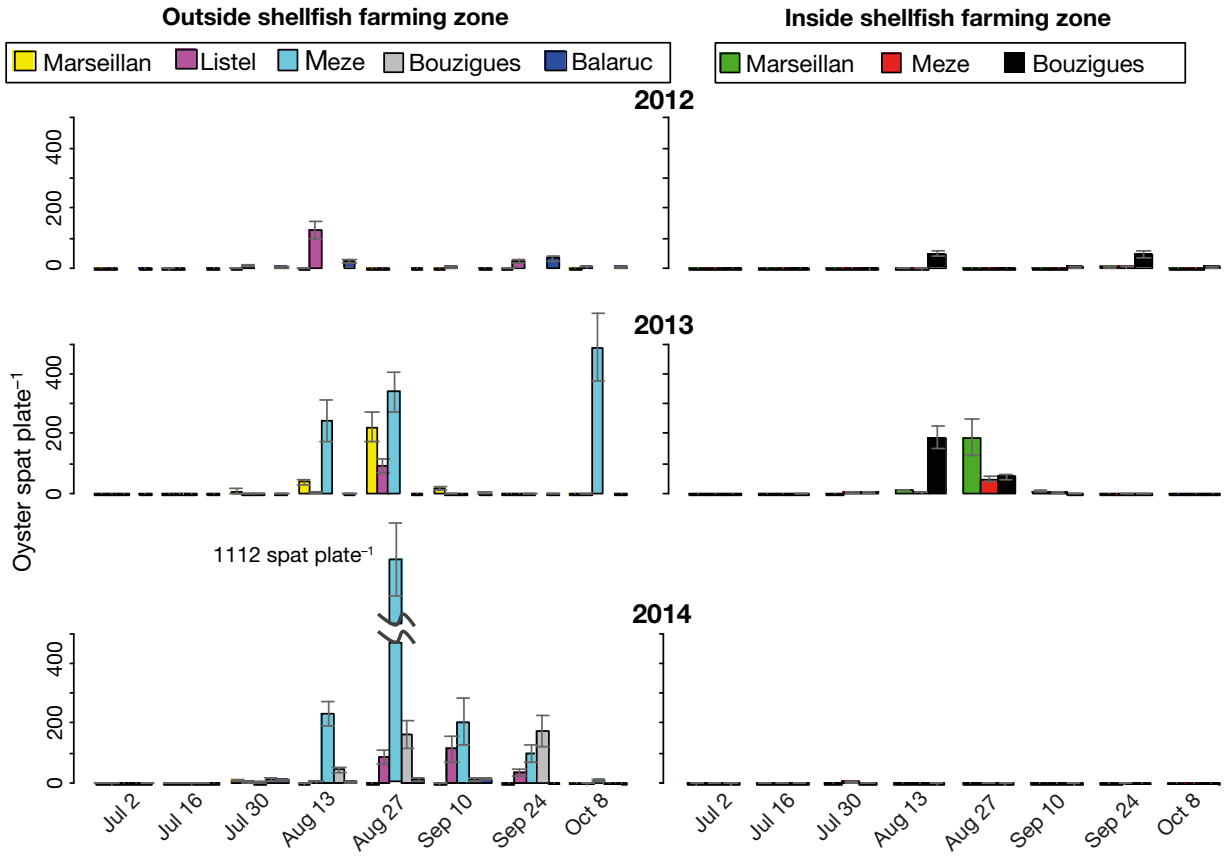

Fig. 6. Mean (±95% confidence intervals) Pacific oyster spat abundance per plate observed at 8 sampling sites in Thau lagoon: 3 located inside the shellfish farming zone and 5 outside. Observations were made at 2 wk intervals throughout the summer in 2012, 2013 and 2014. Spat abundances were estimated after the collector had been immersed for 4 wk (n = 54 per date and sampling site)

at Balaruc_OSFZ on the same date. In 2013, one main spatfall event lasted for 2 consecutive harvests in August, with 244 (13 August) and 341 (28 August) ind. plate^{-1} at Meze_OSFZ, 92 ind. plate^{-1} at Listel_OSFZ (28 August), and 188 (13 August) and 56 (28 August) ind. plate^{-1} at Bouzigues_ISFZ (Fig. 6; 2013). There was a second, even larger spatfall harvest (488 ind. plate^{-1}) that was only detected at Meze_OSFZ on 9 October. The most contrasted results at ISFZ and OSFZ sites were obtained in 2014, with spatfall occurring at all OSFZ sites except Marseillan_OSFZ for a period of 2 mo (Fig. 6; 2014). This period was characterized by 4 consecutive harvest dates between 13 August and 24 September versus no recruitment at all at ISFZ sites. Meze_OSFZ showed the most remarkable spat abundances, peaking at 1112 ind. plate^{-1} on 27 August 2014.

Table 2. ANOVA examining the effect of year, situation (inside or outside the shellfish farming area) and sampling sites on Pacific oyster spat abundance per plate (power Box-Cox transformation; lambda = –0.63, n = 168). Significant values in **bold** ($p < 0.05$)

Factor	df	SS	MS	*F*- value	Pr(>F)
Situation	1	2.44	2.44	8.474	**<0.01**
Site	6	3.99	0.66	2.305	**<0.05**
Year	2	0.05	0.02	0.081	0.922
Situation × year	2	2.06	1.03	3.572	**<0.05**
Site × year	9	3.71	0.41	1.432	0.179
Residuals	147	42.36	0.28		

The mean abundances of D-larvae (across all sampling dates and in all 3 yr) differed significantly with situation (ISFZ vs. OSFZ; $p < 0.0001$) and were higher at ISFZ (7.05×10^4 ind. m^{-3}, n = 46) than OSFZ sites (7.02×10^3 ind. m^{-3}, n = 68) (Fig. 7A). By contrast, the mean abundances of large umbo larvae did not differ statistically ($p > 0.05$) at ISFZ (1.11×10^2 ind. m^{-3}, n = 66) and OSFZ sites (0.89×10^2 ind. m^{-3}, n = 79); median values were also the same (~100 ind. m^{-3}) (Fig. 7B).

Mean abundances of pediveligers differed significantly ($p < 0.0001$) between ISFZ and OSFZ sites (Fig. 7C), but abundances were lower inside (86 ind.

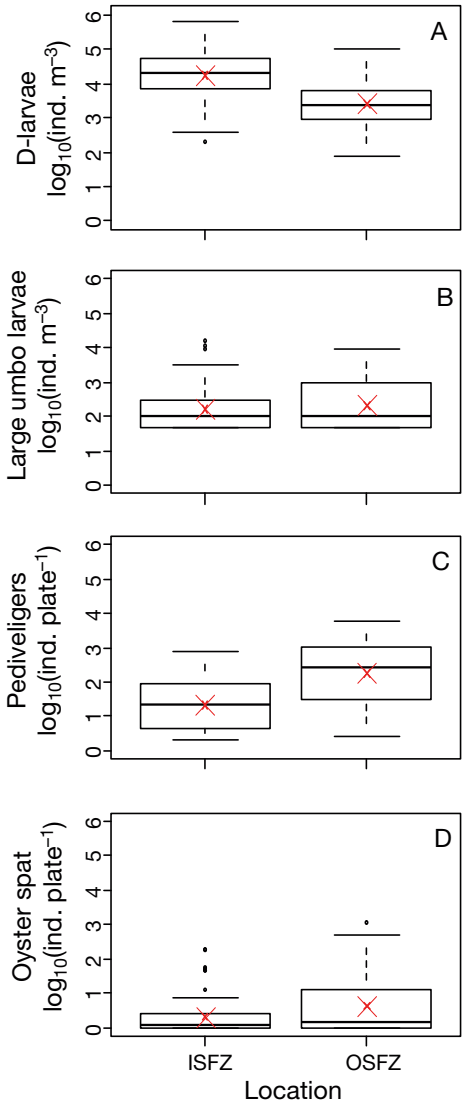

Fig. 7. Distributions of oyster (A) D-larvae (n_{ISFZ} = 46 ; n_{OSFZ} = 68), (B) large umbo larvae (n_{ISFZ} = 66 ; n_{OSFZ} = 79), (C) pediveliger larvae (n_{ISFZ} = 46; n_{OSFZ} = 68) and (D) spat (n_{ISFZ} = 72; n_{OSFZ} = 96) inside (ISFZ) and outside (OSFZ) the shellfish farming zones of Thau lagoon. Mid-line: median; box: 25th and 75th percentiles; whiskers: 1.5 × the interquartile range; circles: outliers; red crosses: means

plate^{-1}, n = 46) than outside (881 ind. plate^{-1}, n = 68). Mean oyster spat abundances were significantly lower at ISFZ ($p < 0.0001$; 9 ind. plate^{-1}, n = 72) than OSFZ sites (42 ind. plate^{-1}; n = 96) (Fig. 7D).

3.2. Spatial patterns of simulated connectivity

The spatial distributions of the CI over Thau lagoon (Fig. 8) for passive tracers released over the oyster farming zones differed significantly depending on the sampling sites ($p < 0.001$; Table 3). The CI was low all along the margins of the lagoon and 2 gradients of increasing values (1) from inside to outside the shellfish farming zone and (2) from west to east elsewhere, with low interannual variability (Table 4).

There was a significant difference between groups of sampling sites at the levels of connectivity with shellfish farming zone (ANOVA, Tukey contrasts multiple comparison tests, $p < 0.001$; Table 4). The lowest mean CI was measured at the 2 most peripheral sites, Balaruc_OSFZ (CI = 0.003 d^{-1}, n = 17) and Marseillan_OSFZ (CI = 0.002 d^{-1}, n = 17) (Fig. 9). By contrast, Bouzigues_ISFZ (CI = 0.008 d^{-1}, n = 16) and Bouzigues_OSFZ (CI = 0.009 d^{-1}, n = 6) had the highest connectivity values. The 4 remaining sites had intermediate connectivity levels, ranging from 0.004–0.007, and were grouped differently (Fig. 9b,c,d groups) by the multiple comparison test depending either on their location along the east–west axis of the lagoon or whether they were located inside or outside the shellfish farming zones.

3.3. Connectivity and larval supply

When we linked observed larval abundances and the CI inside or outside the shellfish farming zones, we found a non-significant relationship ($p > 0.05$; Table 5) between large umbo larvae abundance and connectivity inside and outside the zones (Fig. 10A). The 2 eastern and western sides, Marseillan_OSFZ and Balaruc_OSFZ, had the lowest connectivity and the lowest abundances of large umbo larvae. There was a non-significant difference in the abundances of large umbo larvae with situation ($p > 0.05$; Table 5), with very low depletion at ISFZ sites compared to OSFZ. In contrast, the connectivity index × situation interaction was significant ($p < 0.005$; Table 6) with a significant positive relationship between connectivity and pediveliger abundances at OSFZ sites ($p < 0.0001$; Table 6) whereas for ISFZ sites, this relationship was not significant (Fig. 10B). Only 2 sites (Bouzigues_OSFZ and Marseillan_OSFZ) differed significantly from each other in large umbo larvae abundances (Table 7). The Bouzigues_OSFZ site was defined by high values of connectivity and by high mean abundances of pediveligers (group e, 2291 ind. plate^{-1}; Table 8). With a similar level of connectivity, the Bouzigues_ISFZ site had a mean abundance of pediveligers 70 times lower (group ac, Bouzigues_ISFZ = 28 ind. plate^{-1}). The western sites Marseillan_ISFZ and Marseillan_OSFZ were

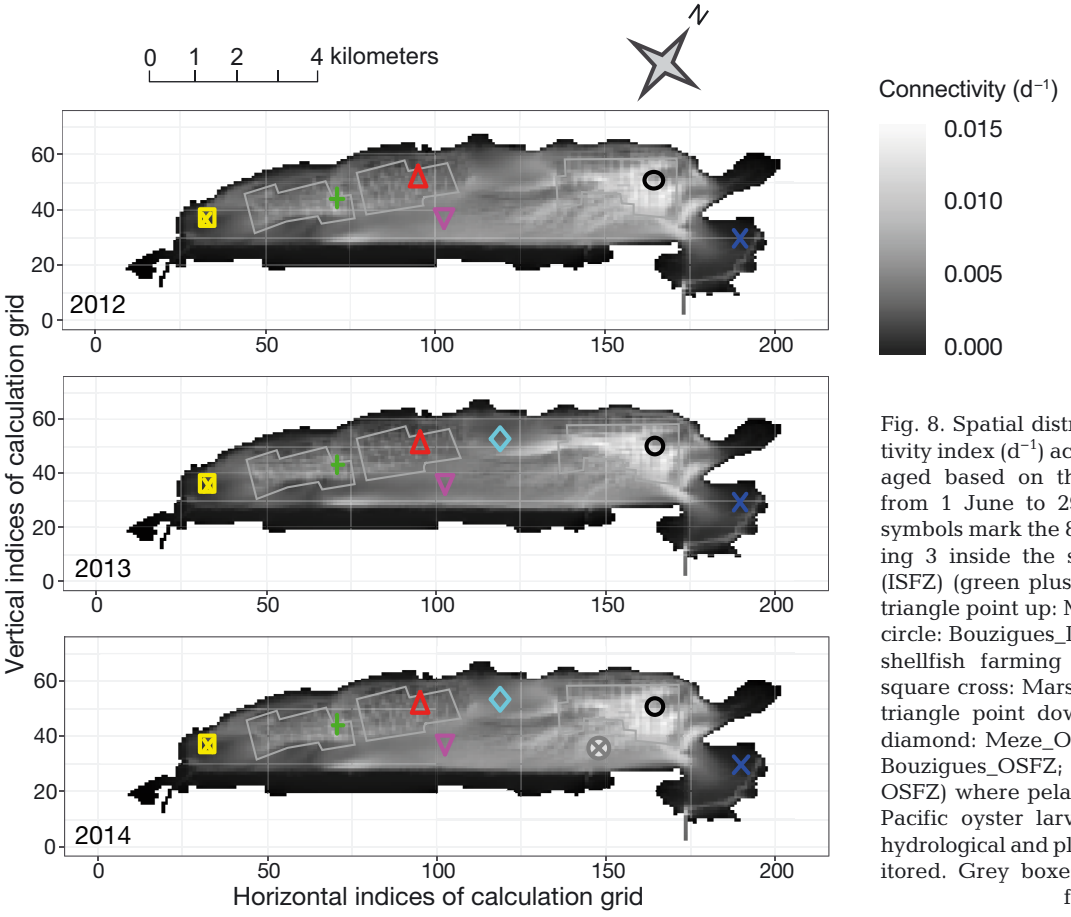

Fig. 8. Spatial distribution of the connectivity index (d^{-1}) across Thau lagoon averaged based on the 50 simulations run from 1 June to 29 September. Colored symbols mark the 8 sampling sites including 3 inside the shellfish farming zone (ISFZ) (green plus: Marseillan_ISFZ; red triangle point up: Meze_ISFZ; black open circle: Bouzigues_ISFZ) and 5 outside the shellfish farming zone (OSFZ) (yellow square cross: Marseillan_OSFZ; magenta triangle point down: Listel_OSFZ; cyan diamond: Meze_OSFZ; grey circle cross: Bouzigues_OSFZ; blue cross: Balaruc_OSFZ) where pelagic larvae and benthic Pacific oyster larvae, spat abundances, hydrological and plankton data were monitored. Grey boxes: location of shellfish farms

characterized by low abundances of pediveligers (respectively, group a and ab, 17 and 28 ind. $plate^{-1}$). In the central part of the lagoon, the pediveliger abundances were approximately 30 times higher at Listel_OSFZ than at Meze_ISFZ (group ab, 22.4 ind. $plate^{-1}$). A ratio of 70 was found between the pediveliger abundances at the site with the highest (Bouzigues_ISFZ) and lowest connectivity (Marseillan_OSFZ). Regarding intercepts of fitted regression models, ISFZ sites such as Bouzigues_ISFZ, Meze_ISFZ and Marseillan_ISFZ had significantly lower pediveliger abundances (20 ind. $plate^{-1}$; $p < 0.05$) than OSFZ sites (204 ind. $plate^{-1}$; $p < 0.001$).

Table 3. ANOVA model examining the effect of sampling sites on the connectivity index. Significant values are in **bold** ($p < 0.05$)

Factor	df	SS	MS	*F*-value	Pr(>F)
Site	7	0.0005	0.00007	57.76	**<0.001**
Residuals	106	0.0001	0.000001		

3.4. Spatial variability of ecological parameters and interactions with pediveliger abundance

The analysis of the multiple regression model linking the abundance of pediveligers to the variables of the planktonic environment explained 69% of the quality of the model fit (Table 9). A significant positive relationship was found for abundances of cyanophycae ($p < 0.05$; Fig. 11A), diatoms ($p < 0.05$; Fig. 11B, Table 9), heterotrophic flagellates ($p < 0.05$; Fig. 11C, Table 9) and nanophytoplankton ($p < 0.05$; Fig. 11D, Table 9). On the contrary, a significant negative relationship was found for abundances of picoeukaryotes ($p < 0.05$; Fig. 11E, Table 9) and Tintinnidae ($p < 0.001$; Fig. 11F, Table 9).

More generally, at the lagoon scale, 8 of the 26 monitored environmental variables (Table 1) differed significantly (Kruskal-Wallis tests, $p < 0.05$) at 3 sampling stations (Marseillan_ISFZ, Bouzigues_ISFZ and Listel_OSFZ): biomasses of pico + nanophytoplankton (<20 µm), microphytoplankton (>20 µm) and nanophytoplankton (3–20 µm) as well as abundances of autotrophic picoeukaryotes, nanophytoplankton, *Chaetoceros* spp., mesozooplankton,

Table 4. Simultaneous tests for general linear hypotheses with Tukey contrasts multiple comparisons of means, fitted on an ANOVA model to examine the effect of Pacific oyster sampling sites on the connectivity index. Linear hypothesis components are site names (ISFZ: inside shellfish farming zone; OSFZ: outside shellfish farming zone; see Fig. 1 for site locations); p-values in **bold** are significant at the 95% confidence level

Linear hypotheses	Estimate	SE	T-value	Pr(>T)
Marseillan_ISFZ – Marseillan_OSFZ = 0	0.00378	0.0004	9.686	**<0.001**
Listel_OSFZ – Marseillan_OSFZ = 0	0.00436	0.0004	11.341	**<0.001**
Meze_ISFZ – Marseillan_OSFZ = 0	0.00198	0.0004	5.144	**<0.001**
Meze_OSFZ – Marseillan_OSFZ = 0	0.00265	0.0004	6.297	**<0.001**
Bouzigues_OSFZ – Marseillan_OSFZ = 0	0.00656	0.0005	12.395	**<0.001**
Bouzigues_ISFZ – Marseillan_OSFZ = 0	0.00578	0.0004	14.019	**<0.001**
Balaruc_OSFZ – Marseillan_OSFZ = 0	0.00038	0.0004	1.004	0.9722
Listel_OSFZ – Marseillan_ISFZ = 0	0.00058	0.0004	1.510	0.7970
Meze_ISFZ – Marseillan_ISFZ = 0	–0.0018	0.0004	–4.688	**<0.001**
Meze_OSFZ – Marseillan_ISFZ = 0	–0.0011	0.0004	–2.671	0.1402
Bouzigues_OSFZ – Marseillan_ISFZ = 0	0.0028	0.0005	5.242	**<0.001**
Bouzigues_ISFZ – Marseillan_ISFZ = 0	0.0020	0.0004	4.847	**<0.001**
Balaruc_OSFZ – Marseillan_ISFZ = 0	0.0034	0.0004	–8.828	**<0.001**
Meze_ISFZ – Listel_OSFZ = 0	–0.0024	0.0004	–6.293	**<0.001**
Meze_OSFZ – Listel_OSFZ = 0	–0.0017	0.0004	–4.100	**0.0018**
Bouzigues_OSFZ – Listel_OSFZ = 0	0.0022	0.0005	4.177	**0.0015**
Bouzigues_ISFZ – Listel_OSFZ = 0	0.0014	0.0004	3.485	**0.0154**
Balaruc_OSFZ – Listel_OSFZ = 0	–0.0040	0.0004	–10.498	**<0.001**
Meze_OSFZ – Meze_ISFZ = 0	0.0007	0.0004	1.625	0.7296
Bouzigues_OSFZ – Meze_ISFZ = 0	0.0046	0.0005	8.723	**<0.001**
Bouzigues_ISFZ – Meze_ISFZ = 0	0.0038	0.0004	9.344	**<0.001**
Balaruc_OSFZ – Meze_ISFZ = 0	–0.0016	0.0004	–4.205	**0.0014**
Bouzigues_OSFZ – Meze_OSFZ = 0	0.0039	0.0005	7.058	**<0.001**
Bouzigues_ISFZ – Meze_OSFZ = 0	0.00312	0.0004	7.069	**<0.001**
Balaruc_OSFZ – Meze_OSFZ = 0	–0.0023	0.0004	–5.450	**<0.001**
Bouzigues_ISFZ – Bouzigues_OSFZ = 0	–0.0008	0.0005	–1.417	0.8444
Balaruc_OSFZ – Bouzigues_OSFZ = 0	–0.0062	0.0005	–11.760	**<0.001**
Balaruc_OSFZ – Bouzigues_ISFZ = 0	–0.0054	0.0004	–13.258	**<0.001**

competitors and predators (Fig. 12). Generally, abundances and biomasses were lowest at Marseillan_ISFZ, intermediate at Bouzigues_ISFZ and highest at Listel_OSFZ, except picoeukaryote abundances which were lowest at Listel_OSFZ. Significant differences were found in 5 of the 26 variables (pico + nanophytoplankton biomass, nanophytoplankton biomass, microphytoplankton biomass, *Chaetoceros* spp. abundance and predator abundance) between the 2 ISFZ sites, with lower values at Marseillan than at Bouzigues. The averaged biomass of pico + nanophytoplankton was lower at Marseillan_ISFZ (0.87 ± 0.33 µg chl *a* l^{-1}) than at Bouzigues_ISFZ (1.14 ± 0.45 µg chl *a* l^{-1}) as $nanophytoplankton_{Marseillan\_ISFZ}$ (0.44 ± 0.27 µg chl *a* l^{-1}) and $nanophytoplankton_{Bouzigues\_ISFZ}$ (0.71 ± 0.37 µg chl *a* l^{-1}) and $microphytoplankton_{Marseillan\_ISFZ}$ (0.29 ± 0.25 µg chl *a* l^{-1}) and $microphytoplankton_{Bouzigues\_ISFZ}$ (0.82 ± 0.51 µg chl *a* l^{-1}). Abundances of *Chaetoceros* spp. differed between Marseillan_ISFZ and Bouzigues_ISFZ with respectively $4.53 \times 10^4 \pm 9.87 \times 10^4$ cells l^{-1} and $2.13 \times 10^5 \pm 3.22 \times 10^5$ cells l^{-1}. The contrasts between the sites inside and outside the shellfish farming zone were mainly expressed by the abundances of picoeukaryotes, *Chaetoceros* spp., nanophytoplankton, competitors and predators. Abundances of picoeukaryotes were similar at Marseillan_ISFZ ($3.6 \times 10^7 \pm 2.1 \times 10^7$ cells l^{-1}) and Bouzigues_ISFZ ($3.4 \times 10^7 \pm 1.7 \times 10^7$ cells l^{-1}) and almost double those at Listel_OSFZ ($1.8 \times 10^7 \pm 0.9 \times 10^7$ cells l^{-1}). *Chaetoceros* spp. were highly abundant: $4.2 \times 10^5 \pm 5.0 \times 10^5$ cells l^{-1} at Listel_OSFZ, corresponding to 2- and 9-fold higher abundance than that recorded at Bouzigues_ISFZ and at Marseillan_ISFZ, respectively. Nanophytoplankton were 30% more abundant at Listel_OSFZ ($4.0 \times 10^6 \pm 2.36 \times 10^6$ cells l^{-1}) than at Bouzigues_ISFZ ($3.2 \times 10^6 \pm 2.66 \times 10^6$ cells l^{-1}). Competitors were on average twice as abundant at OSFZ sites ($competitors_{Listel\_OSFZ}$ =

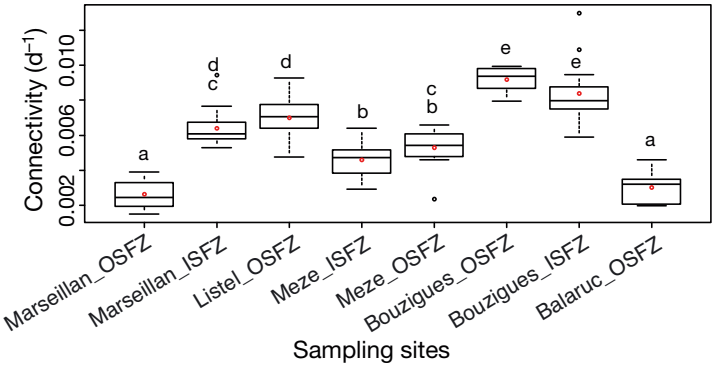

Fig. 9. Simulated connectivity at the experimental sampling sites (see Fig. 1 for site names and locations) on each collector sampling date (n = 132). Different lowercase letters indicate significant differences between groups resulting from a Tukey contrasts multiple comparisons test ($p \leq 0.05$). Mid-line: median; box: 25th and 75th percentiles; whiskers: 1.5 × the interquartile range; red circles: means; black circles: outliers

Table 5. ANCOVA table and summary examining the effect of the connectivity index and situation (i.e. inside or outside the shellfish farming zone [OSFZ]) factors on large Pacific oyster umbo larvae abundance (log_{10} transform) in the water column. Significant values are in **bold** ($p < 0.05$)

Factor	df	SS	MS	*F*-value	Pr(>F)
Connectivity index	1	1.093	1.093	2.586	0.110
Situation	1	0.894	0.894	2.114	0.148
Connectivity index × situation	1	0.072	0.072	0.171	0.680
Residuals	141	59.612	0.423		
Summary		**Estimate**	**SE**	**T-value**	**Pr(>T)**
(Intercept)		2.007	0.276	7.271	**<0.001**
Connectivity index		35.927	41.795	0.860	0.391
Situation[OSFZ]		0.044	0.320	0.138	0.891
Connectivity index × situation[OSFZ]		21.457	51.937	0.413	0.680
Residual SE	0.650 on 141 df				
Multiple R^2	0.033		Adjusted R^2	0.0128	
F-statistic	1.623 on 3 and 141 df		p-value	0.187	

4. DISCUSSION

The aim of this study was to evaluate the processes that drive spatial patterns of larval supply, settlement and recruitment of the Pacific oyster in a Mediterranean nanotidal semi-enclosed coastal lagoon. The results of the 3 yr study revealed marked variability of observed oyster recruitment at the lagoon scale, including high and low abundance of spat after collections. This variability reflects the ecological heterogeneity of Thau lagoon. In previous studies, Lagarde et al. (2017, 2018) showed that the temporal variability of recruitment was related to lagoon functioning driven by temperature and trophic inputs (abundance of nanophytoplankton and *Chaetoceros* spp.). The spatial heterogeneity measured in the present study suggests that different hydrodynamic and ecological processes occur simultaneously at sampling sites located in the east vs. west and inside vs. outside the shellfish farming zones. The sampling sites in the east and west parts of the lagoon showed the lowest recruitment while the spatial windows most favorable for recruitment were located in the

$36.1 \times 10^3 \pm 28.5 \times 10^3$ ind. m^{-3}) than at ISFZ (competitors$_{Bouzigues_ISFZ}$ = $18.6 \times 10^3 \pm 12.8 \times 10^3$ ind. m^{-3}; competitors$_{Marseillan_ISFZ}$ = $20.3 \times 10^3 \pm 17.0 \times 10^3$ ind. m^{-3}). Predator abundance was lower at ISFZ sites (predators$_{Marseillan_ISFZ}$ = 0.05 ± 0.06 ind. m^{-3}; predators$_{Bouzigues_ISFZ}$ = 0.19 ± 0.22 ind. m^{-3}) than at OSFZ sites (predators$_{Listel_OSFZ}$ = 0.46 ± 0.44 ind. m^{-3}).

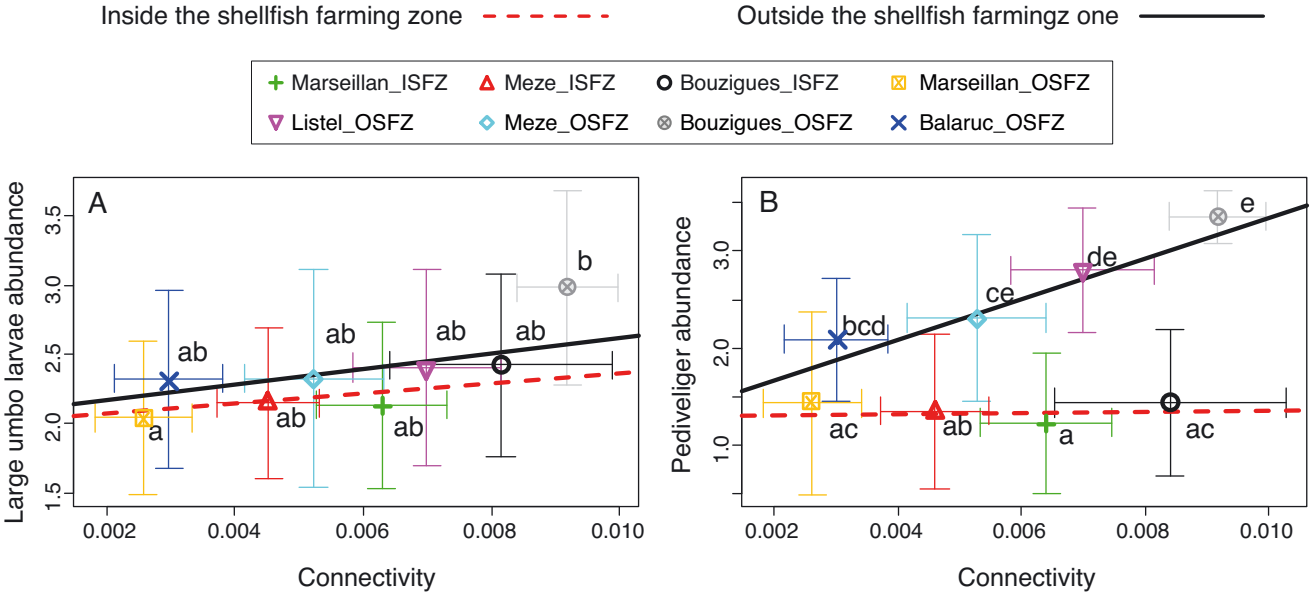

Fig. 10. Relationship between connectivity (mean ± SE) and abundance of (A) large Pacific oyster umbo larvae (log_{10} m^{-3}, n_{ISFZ} = 66, n_{OSFZ} = 79) and (B) pediveligers (log_{10} $plate^{-1}$, n_{ISFZ} = 46, n_{OSFZ} = 68) at the 8 sampling sites; 3 inside (ISFZ) and 5 outside (OSFZ) the shellfish fishing zone. Black line: OSFZ linear regression line; red dashed line: ISFZ linear regression line. Letters differentiate the level of the group according to the Tukey contrasts multiple comparisons of means

Table 6. ANCOVA table and summary examining the effect of the connectivity index and situation (i.e. inside or outside the shellfish farming zone [OSFZ]) factors on Pacific oyster pediveliger abundance (log_{10} transform) in collectors. Significant values are in **bold** ($p < 0.05$)

Factor	df	SS	MS	*F*-value	Pr(>F)
Connectivity index	1	3.286	3.286	5.4130	**<0.05**
Situation	1	32.510	32.510	53.554	**<0.001**
Connectivity index × situation	1	5.009	5.009	8.251	**<0.005**
Residuals	110	66.775	0.607		
Summary		**Estimate**	**SE**	**T-value**	**Pr(>T)**
(Intercept)		1.294	0.3855	3.356	**<0.01**
Connectivity index	6.410	58.406	0.110	0.9128	
Situation[OSFZ]	−0.042	0.441	−0.095	0.9244	
Connectivity index × situation[OSFZ]		202.592	70.530	2.872	**<0.01**
Residual SE	0.779 on 110 df				
Multiple R^2	**0.3793**		Adjusted R^2		**0.362**
F-statistic	22.4 on 3 and 110 df		p-value		**<0.001**

center of the lagoon, outside the shellfish farmed zone.

There is negligible wild Pacific oyster broodstock in the coastal Thau lagoon, thus larvae were mainly collected from reared oyster stock inside the shellfish farming zones. We hypothesize that restricted nanotidal lagoons promote larval retention due to the characteristics of the enclosed lagoon and that the nanotidal regime has limited effects. In this context, the emergence of D-larvae cohorts after adult spawning events determines the larval supply to the system. The abundances of D-larvae at ISFZ sites were higher than at OSFZ sites, confirming that the D-larvae came from the oyster rearing areas. The abundances of large umbo larvae were similar inside and outside shellfish farming zone, likely due to the combined effects of high larval retention and hydrodynamic currents, the driving forces of both dispersion and connectivity in Thau lagoon.

However, the temporal variability of the phenomenon is highlighted by the high maximum concentrations of large umbo larvae recorded in Thau lagoon in 2010 and 2011, with respectively 6100 and 55 000 larvae m^{-3} (Rayssac et al. 2012), whereas in 2012, 2013 and 2014, the maximum concentrations only reached respectively 160, 450 and 27 larvae m^{-3}. For the sake of comparison, in 2013, the maximum concentrations of large umbo larvae were 120 larvae m^{-3} in the Arcachon basin and 29 larvae m^{-3} in the Marennes-Oléron basin (Pouvreau et al. 2013, 2015). In Thau lagoon, the supply of pelagic larvae was guaranteed by the high density of oyster broodstock (Gangnery et al. 2004) and the self-recruitment ability of the enclosed basin. Given the homogeneous high abundances of pelagic large umbo larvae, we conclude

Table 7. Simultaneous tests for general linear hypotheses with Tukey contrasts multiple comparisons of means, fitted on an ANOVA model to examine the effect of sampling sites on large Pacific oyster umbo larvae abundance. Linear hypotheses components are site names (ISFZ: inside shellfish farming zone; OSFZ: outside shellfish farming zone; see Fig. 1 for site locations); p-values in **bold** are significant at the 95% confidence limit

Linear hypotheses	Estimate	SE	T-value	Pr(>T)
Marseillan_ISFZ − Marseillan_OSFZ = 0	0.089	0.197	0.452	0.999
Listel_OSFZ − Marseillan_OSFZ = 0	0.360	0.202	1.782	0.625
Meze_ISFZ − Marseillan_OSFZ = 0	0.103	0.197	0.525	0.999
Meze_OSFZ − Marseillan_OSFZ = 0	0.280	0.228	1.231	0.919
Bouzigues_OSFZ − Marseillan_OSFZ = 0	0.938	0.297	3.154	**<0.05**
Bouzigues_ISFZ − Marseillan_OSFZ = 0	0.378	0.197	1.915	0.535
Balaruc_OSFZ − Marseillan_OSFZ = 0	0.278	0.202	1.375	0.862
Listel_OSFZ − Marseillan_ISFZ = 0	0.271	0.197	1.372	0.864
Meze_ISFZ − Marseillan_ISFZ = 0	0.014	0.192	0.074	1.000
Meze_OSFZ − Marseillan_ISFZ = 0	0.191	0.224	0.854	0.989
Bouzigues_OSFZ − Marseillan_ISFZ = 0	0.849	0.294	2.884	0.080
Bouzigues_ISFZ − Marseillan_ISFZ = 0	0.289	0.193	1.499	0.801
Balaruc_OSFZ − Marseillan_ISFZ = 0	0.189	0.197	0.955	0.978
Meze_ISFZ − Listel_OSFZ = 0	−0.256	0.197	−1.299	0.894
Meze_OSFZ − Listel_OSFZ = 0	−0.080	0.228	−0.351	1.000
Bouzigues_OSFZ − Listel_OSFZ = 0	0.578	0.297	1.943	0.515
Bouzigues_ISFZ − Listel_OSFZ = 0	0.018	0.197	0.091	1.000
Balaruc_OSFZ − Listel_OSFZ = 0	−0.082	0.202	−0.407	0.999
Meze_OSFZ − Meze_ISFZ = 0	0.176	0.223	0.790	0.993
Bouzigues_OSFZ − Meze_ISFZ = 0	0.834	0.294	2.836	0.091
Bouzigues_ISFZ − Meze_ISFZ = 0	0.274	0.193	1.424	0.839
Balaruc_OSFZ − Meze_ISFZ = 0	0.174	0.197	0.883	0.986
Bouzigues_OSFZ − Meze_OSFZ = 0	0.658	0.315	2.086	0.420
Bouzigues_ISFZ − Meze_OSFZ = 0	0.098	0.223	0.438	0.999
Balaruc_OSFZ − Meze_OSFZ = 0	−0.002	0.228	−0.010	1.000
Bouzigues_ISFZ − Bouzigues_OSFZ = 0	−0.560	0.294	−1.903	0.542
Balaruc_OSFZ − Bouzigues_OSFZ = 0	−0.660	0.297	−2.220	0.339
Balaruc_OSFZ − Bouzigues_ISFZ = 0	−0.100	0.197	−0.507	0.999

Table 8. Simultaneous tests for general linear hypotheses with Tukey contrasts multiple comparisons of means, fitted on an ANOVA model to examine the effect of sampling sites on Pacific oyster pediveliger abundance. Linear hypotheses components are site names (ISFZ: inside shellfish farming zone; OSFZ: outside shellfish farming zone; see Fig. 1 for site locations); p-values in **bold** are significant at the 95% confidence level

Linear hypotheses	Estimate	SE	T-value	Pr(>T)
Marseillan_ISFZ – Marseillan_OSFZ = 0	–0.208	0.265	–0.782	0.993
Listel_OSFZ – Marseillan_OSFZ = 0	1.367	0.261	5.225	**<0.01**
Meze_ISFZ – Marseillan_OSFZ = 0	–0.085	0.261	–0.326	1.000
Meze_OSFZ – Marseillan_OSFZ = 0	0.877	0.286	3.057	0.053
Bouzigues_OSFZ – Marseillan_OSFZ = 0	1.919	0.359	5.337	**<0.01**
Bouzigues_ISFZ – Marseillan_OSFZ = 0	0.002	0.280	0.007	1.000
Balaruc_OSFZ – Marseillan_OSFZ = 0	0.651	0.261	2.492	0.206
Listel_OSFZ – Marseillan_ISFZ = 0	1.574	0.261	6.019	**<0.01**
Meze_ISFZ – Marseillan_ISFZ = 0	0.122	0.261	0.468	0.999
Meze_OSFZ – Marseillan_ISFZ = 0	1.084	0.286	3.781	**<0.01**
Bouzigues_OSFZ – Marseillan_ISFZ = 0	2.126	0.359	5.914	**<0.01**
Bouzigues_ISFZ – Marseillan_ISFZ = 0	0.209	0.280	0.748	0.995
Balaruc_OSFZ – Marseillan_ISFZ = 0	0.859	0.261	3.285	**<0.05**
Meze_ISFZ – Listel_OSFZ = 0	–1.452	0.257	–5.637	**<0.01**
Meze_OSFZ – Listel_OSFZ = 0	–0.490	0.283	–1.73	0.661
Bouzigues_OSFZ – Listel_OSFZ = 0	0.551	0.356	1.547	0.775
Bouzigues_ISFZ – Listel_OSFZ = 0	–1.365	0.276	–4.933	<0.01
Balaruc_OSFZ – Listel_OSFZ = 0	–0.715	0.257	–2.776	0.110
Meze_OSFZ – Meze_ISFZ = 0	0.962	0.283	3.397	0.020
Bouzigues_OSFZ – Meze_ISFZ = 0	2.004	0.356	5.619	**<0.01**
Bouzigues_ISFZ – Meze_ISFZ = 0	0.087	0.276	0.316	1.000
Balaruc_OSFZ – Meze_ISFZ = 0	0.737	0.257	2.861	0.089
Bouzigues_OSFZ – Meze_OSFZ = 0	1.042	0.375	2.775	0.109
Bouzigues_ISFZ – Meze_OSFZ = 0	0.874	0.300	–2.909	0.079
Balaruc_OSFZ – Meze_OSFZ = 0	–0.224	0.283	–0.794	0.992
Bouzigues_ISFZ – Bouzigues_OSFZ = 0	–1.917	0.370	–5.171	**<0.01**
Balaruc_OSFZ – Bouzigues_OSFZ = 0	–1.267	0.356	–3.553	**<0.05**
Balaruc_OSFZ – Bouzigues_ISFZ = 0	0.649	0.276	2.348	0.272

that the abundance of pelagic larvae is not a limiting factor for oyster recruitment in Thau lagoon.

In this study, the relatively homogeneous abundances of large umbo larvae inside and outside the shellfish farming zone also suggest the absence of intense larviphagy (Lehane & Davenport 2004, Troost et al. 2008a,b). Thus, although larviphagy probably exists in Thau lagoon, it had only a minor effect on the variability of recruitment.

Larval dispersion through hydrodynamic circulation is considered to be an important process in the recruitment of marine invertebrates (Levin 2006, LeCorre 2013, Ghezzo et al. 2015). The hydrodynamic circulation in coastal lagoons is strongly constrained by the borders, bathymetry and direction and intensity of the wind (Ghezzo et al. 2015, Fiandrino et al. 2017). Our simulation results concerning the connectivity indicator showed that, like the pearl oyster in a Pacific lagoon (Thomas et al. 2016), the distribution of the last pelagic larval stage (umbo larvae) in Thau lagoon tended to be spatially homogeneous. However, cumulative fluxes of tracers revealed significant differences in hydrodynamic connectivity among sites, depending on their location in the lagoon. Low hydrodynamic connectivity is usually found in highly confined sites (Guelorget et al. 1987, Guelorget & Perthuisot 1992) like the western part of Thau lagoon, or areas under the influence of the sea like the eastern part of Thau lagoon. Indeed, the westernmost (Marseillan_OSFZ) and easternmost (Balaruc_OSFZ) sampling sites had the lowest simulated connectivity with oyster farming areas. Conversely, the 2 sampling sites characterized by the highest connectivity (Bouzigues_ISFZ and Bouzigues_OSFZ) are not only influenced by the main Bouzigues oyster zone, but are also located in a zone with preferential gyre patterns (Fiandrino et al. 2017). In a nanotidal restricted lagoon like Thau, gyre circulation is mainly driven by wind and is constrained by topography (bathymetry and sinuosity) (Bernard et al. 2013, Fiandrino et al. 2017). In agreement with Pérez-Ruzafa et al. (2019), our results show that the effects of hydrodynamic connectivity play a key role in the biological and community spatial structure of coastal lagoons.

Comparing simulated hydrodynamic connectivity with observed larval development makes it possible to identify and distinguish the role of hydrodynamics from that of ecological factors during the recruitment process. Overall, our results suggest that at the large umbo stage, larval supply was primarily structured by the presence of shellfish-growing areas nearby, and then by hydrodynamics, with relative homogeneity in the center of the system (Lagarde et al. 2017, 2018). At the ISFZ sites, our results suggest that the reduction in recruitment that occurred was due to loss of settlement competence at the pediveliger stage, leading to a dramatic average 10-fold (up to 70-fold) loss in pediveliger abundance per plate. The heterogeneity of the pediveliger supply can be explained on one hand by connectivity in the OSFZ sites and on the other hand by the effect of the location (ISFZ vs. OSFZ).

Table 9. Analysis of the linear multiple regression between Pacific oyster pediveliger abundance and environmental variables. Significant values ($p < 0.05$) are in **bold.** Superscript A: abundance; superscript B: biomass. Linear model: log10(pediveligeres) ~ Temperature + Salinity + log_HF^{A} + log10.ciliates^{A} + log10.tinti^{A} + sqrt_comp^{A} + log_pred^{A} + log_nano_tot^{A} + log_nano_inf20^{B} + log_micro^{B} + log_pico^{B} + log_peuk_tot^{A} + log_cyan_tot^{A} + log_crypto^{A} + log_diatoms^{A} + log_dinoflagellates^{A} + log_chaetoceros^{A}

Coefficients	Estimate	SE	T-value	p-value
Intercept	−6.927	4.881	−1.419	0.162
Temperature	−0.0278	0.071	−0.392	0.696
Salinity	0.142	0.109	1.296	0.201
log_HF^{A}	0.922	0.416	2.215	**0.031**
log_ciliates^{A}	0.654	0.535	1.223	0.227
log_tinti^{A}	−0.746	0.263	−2.835	**0.006**
sqrt_comp^{A}	0.069	0.086	0.801	0.427
log_pred^{A}	0.075	2.035	0.037	0.970
log_nano_tot^{A}	1.859	0.728	2.551	**0.014**
log_nano_inf20^{B}	−2.349	2.569	−0.914	0.365
log_micro^{B}	−0.5432	1.741	−0.312	0.756
log_pico^{B}	−3.292	5.532	−0.595	0.554
log_peuk_tot^{A}	−1.219	0.604	−2.018	**0.049**
log_cyan_tot^{A}	0.821	0.340	2.415	**0.019**
log_crypto^{A}	−2.282	2.163	−1.055	0.2972
log_diatoms^{A}	0.530	0.247	2.146	**0.037**
log_dinoflagellates^{A}	−0.949	0.499	−1.901	0.063
log_chaetoceros^{A}	−0.094	0.137	−0.686	0.4963
Residual SE	0.7743 on 45 df			
Multiple R^2	**0.691**			
Adjusted R^2	**0.575**			
$F_{17,45}$	5.939			
p	**<0.0001**			

In a previous study, Lagarde et al. (2017) showed that over time, the abundance of pediveligers was driven by the abundance of specific trophic plankton such as the diatoms *Chaetoceros* spp. in this ecosystem, supporting the hypothesis of the trophic settlement trigger (Toupoint et al. 2012). In the present study, significant spatial differences in phytoplankton abundance and biomass were detected between shellfish farming sites Bouzigues_ISFZ in the eastern part of the lagoon and Marseillan_ISFZ in the western part. This east–west gradient was shown to be due to nutrient inputs (the main inputs come from perennial rivers entering the lagoon in the east) (Jarry et al. 1990, Plus et al. 2006) and was amplified by the filter-feeders' trophic depletion of phytoplankton biomass, with 1.7-fold more nanophytoplankton and 2.8-fold more microphytoplankton at the eastern site Bouzigues_ISFZ than at the western site Marseillan_ISFZ. Similarly, regarding phytoplankton abundance, almost 5 times more *Chaetoceros* spp. were counted at Bouzigues_ISFZ than at Marseillan_ISFZ. The contrast between ISFZ and OSFZ sites was underlined by twice as many picoeukaryote counted inside than outside. Abundances of *Chaetoceros* spp. were twice as high at Listel_OSFZ than at Bouzigues_ISFZ, and 9-fold higher at Marseillan_ISFZ. Nanophytoplankton were 30% more abundant at Listel_OSFZ than at the ISFZ sites. As we showed a positive effect of cyanophycae, diatoms, heterotrophic flagellates and nanophytoplankton on pediveliger abundance, we hypothesize that the loss of settlement competence of pediveligers inside the oyster rearing zones is linked to the depletion of food resources (i.e. nanophytoplankton and diatoms), thereby reducing the effect of the trophic settlement trigger. A decrease in the abundance of oyster spat was observed both ISFZ and OSFZ compared to the abundance of pediveligers, suggesting a low survival rate at metamorphosis, both at ISFZ and OSFZ sites. We previously showed that survival at metamorphosis was positively correlated with nanophytoplankton abundance (Lagarde et al. 2017). Other authors demonstrated that the presence of shellfish results in a decrease in zooplankton and phytoplankton biomasses, with deficits of 30 and 40% respectively (Lam-Hoai et al. 1997, Souchu et al. 2001, Bec et al. 2005). In line with these results, we observed that nanophytoplankton abundance was lower at ISFZ sites than at OSFZ sites. This depletion is due to trophic filtration (top-down control inside the shellfish farming zones) of adult shellfish, including oysters (Deslous-Paoli et al. 1993, Pernet et al. 2012, Lagarde et al. 2017), with an indirect impact on pediveliger abundances, metamorphosis, survival and spat abundance. We therefore conclude that feeding constraints during sensitive stages such as settlement and metamorphosis were responsible for the heterogeneous recruitment observed at the scale of the whole lagoon.

Zooplanktonic trophic competitors and potential predators in the water column mirrored the population dynamics of autotrophic prey and that of the oyster larvae without significantly or negatively impacting oyster recruitment (Lagarde et al. 2017). In our previous study, we showed that there was no negative correlation between recruitment and the abundance of predators and/or competitors. In the case of competitors, our results suggest that their abundances are lower ISFZ than OSFZ because the filtration pressure of the adult oysters exerts top-down control of the trophic chain.

Our results suggest that the disruption of the supply of pediveligers is due to lack of food (trophic competition, and lack of energy) or unsuit-

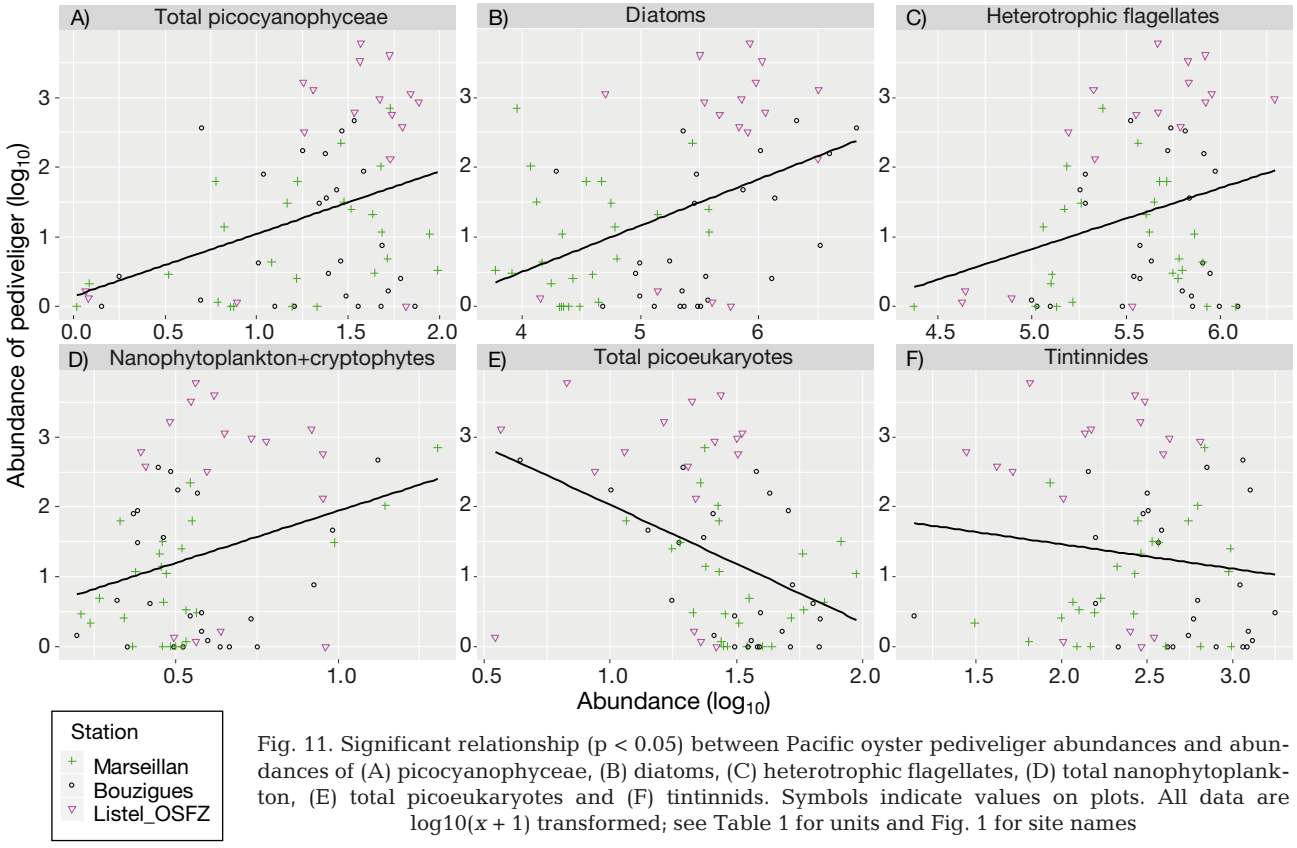

Fig. 11. Significant relationship ($p < 0.05$) between Pacific oyster pediveliger abundances and abundances of (A) picocyanophyceae, (B) diatoms, (C) heterotrophic flagellates, (D) total nanophytoplankton, (E) total picoeukaryotes and (F) tintinnids. Symbols indicate values on plots. All data are log10(x + 1) transformed; see Table 1 for units and Fig. 1 for site names

able food (tintinnids, picoeukaryotes) leading to energy-deficient larvae.

In the case of picoeukaryotes, abundances at 2 ISFZ sites (Marseillan_ISFZ and Bouzigues_ISFZ) were higher than the OSFZ site Listel_OSFZ. This suggests that while filter feeders (such as oysters and mussels in the farms) affect the biomass and abundance of nano- and microplankton, they have much less impact on picoplankton, as they are not able to directly retain the smaller particles (Vaquer et al. 1996, Dupuy et al. 2000, Lefebvre et al. 2000). Moreover, picoplankton abundances increase through a feedback loop i.e. the excretion of cultured bivalves favors the microbial loop based on smaller phytoplankton (Bec et al. 2005) and provides for top-down trophic control inside the shellfish farming zone (Lagarde et al. 2017, 2018). Top-down trophic control has already been hypothesized based on observed spatial depletion of plankton, including secondary producers (Lam-Hoai et al. 1997), or by comparing different shellfish exploited areas over time (Lagarde et al. 2017, 2018). Some complementary diagnoses provided by the 'median lagoon-scale depletion index' based on modeling carrying capacity (Filgueira et al. 2014) revealed negative values of the index in summer and at the beginning of autumn (Pete et al. unpubl. data). These authors used Dame's index (Dame & Prins 1998) based on excess primary production integrated over the year to demonstrate the direct influence of shellfish farming on phytoplankton resources inside the shellfish farming zone. Regarding Thau lagoon, the production of shellfish appeared to be negatively correlated with the depletion index (Pete et al. unpubl. data).

Our hypothesis that oyster larvae at ISFZ sites of Thau lagoon suffer from food depletion challenges the claim that food limitation is seldom important for invertebrate larvae (Olson & Olson 1989). These authors argued that food limitation is more common in the open ocean than in nearshore waters. Our results suggest that bivalve recruitment in coastal lagoons is negatively impacted by trophic competition during trophic top-down control in summer, particularly in the case of highly exploited shellfish farming ecosystem under oligotrophication process.

Successful recruitment of juveniles to an existing bivalve population depends on substrate preferences and interspecific interactions. To standardize our collection, sampling sites were all equipped with the same type of plate collectors (coupelles) to enable us

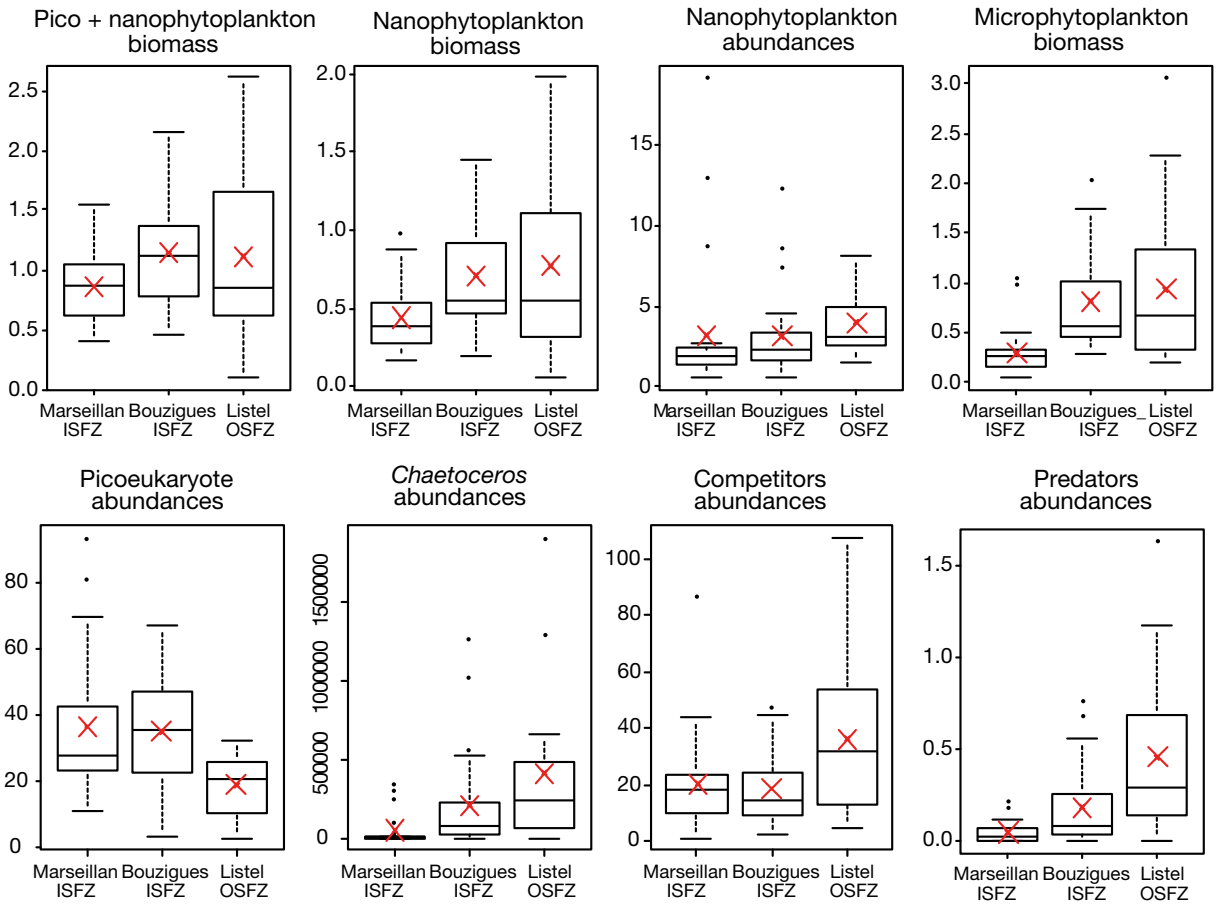

Fig. 12. Plankton abundances that revealed a significant difference ($p < 0.05$) among sampling sites Marseillan_ISFZ ($n_{Marseillan\_ISFZ} = 25$), Bouzigues_ISFZ ($n_{Bouzigues\_ISFZ} = 25$) and Listel_OSFZ ($n_{Listel\_OSFZ} = 17$), inside (ISFZ) and outside (OSFZ) the shellfish farming zones of Thau lagoon (see Fig. 1 for site names and locations). See Fig. 7 for definitions of plots. Nanophytoplankton and picoeukaryotes abundances: in 10^6 cells l^{-1}; *Chaetoceros* spp.: cells l^{-1}; competitors: 10^3 ind. m^3; predators: $\log_{10}$ ind. m^3

to compare intra-lagoon and inter-basin recruitment, particularly in the framework of the French Oyster Larvae Monitoring Network (Pouvreau et al. 2018). Spat collection on collector plates differs from natural recruitment. In particular, it is not certain that predators have the same access to spat on collector plates as on natural substrate. After recruitment (as defined here), the interspecific interactions that take place on the collectors have a strong effect on benthic assemblages. The next step will be to characterize benthic assemblages to define the type of interaction (predation, trophic or territorial competition) using a probabilistic model of species co-occurrence (Veech 2013, Griffith et al. 2016) and to obtain more details on the functioning of the ecosystem in the context of oligotrophication and global climate change. This approach will also make it possible to qualify ecological functions such as the 'oyster nursery' in Thau lagoon.

This study of the spatial patterns of recruitment and connectivity completes the recent discovery of oyster spatfields in Thau lagoon (Lagarde et al. 2017, 2018). Confirmation of spatfields outside shellfish growing areas in this ecosystem, with levels of collection never measured to date, opens new prospects for nurseries of locally born Pacific oyster juveniles. In the context of climate change, the challenge will be to help the bivalve sectors reduce their environmental footprint as suggested by Aubin et al. (2018); improvements still have to be proposed with respect to energy demands to reduce e.g. fuel consumption linked to transport. One way to achieve this goal is to promote and select local strains of cupped oyster that are better adapted to the local farming ecosystem. Another advantage of local development is reducing risks associated with transfer, as moving shellfish within and between countries and ecosystems implies a high risk of ecological impacts (ICES 2011). Along with the target shellfish, transfers can introduce associated organisms (e.g. non-indigenous species, fouling organisms), potentially toxic algae,

pathogens (viruses, bacteria, parasites) or the same species with a different genetic makeup (Brenner et al. 2014, Carnegie et al. 2016). Local alternatives e.g. hatcheries or spat collection methods should be investigated before consideration of transfers as a last resort (Brenner et al. 2014).

The method we presented in this paper could be transposed to other basins or other species such as clams, mussels or scallops to better understand the spatial patterns of oyster recruitment or, more globally, bivalve recruitment, to improve their collection and to draw up recommendations to enable the industrial sector to develop a sustainable activity. It could be integrated in Marine Spatial Planning tools designed to explore shellfish carrying capacity (Filgueira et al. 2015, Bacher et al. 2019). These scientific inputs should prove useful in supporting the blue economic development of a marine culture sector through the righteous practice of natural oyster collection according to sustainable uses in an ecosystem currently undergoing oligotrophication, ecological restoration and global change.

Acknowledgements. The authors thank the funders of the project 'PRONAMED 2': France-Agrimer, Conseil Régional d'Occitanie/Languedoc-Roussillon, Conseil départemental de l'Hérault, Comité Régional de la Conchyliculture en Méditerranée, Cepralmar and Ifremer. F.L. and T.G. thank the RECHAGLO international research group for encouragement, support, and exchanges with Canada. Our special thanks to Adeline Perignon, Erika Gervasoni, Hélène Cochet and Cochet-Environnement, Jean-Louis Guillou, Patrik Le Gall, Gregory Messiaen, Marine Fuhrmann, Marie Boj, Slem Meddah, Solen Soriano and Axel Leurion for their assistance, their involvement and commitment during field and laboratory work. The authors also thank Luke Poirier, a native English scientific researcher, for proofreading the manuscript.

LITERATURE CITED

Arakawa KY (1990) Competitors and fouling organisms in the hanging culture of the pacific oyster, *Crassostrea gigas* (Thunberg). Mar Behav Physiol 17:67–94

Aubin J, Fontaine C, Callier M, Roque d'orbcastel E (2018) Blue mussel (*Mytilus edulis*) bouchot culture in Mont-St Michel Bay: potential mitigation effects on climate change and eutrophication. Int J Life Cycle Assess 23: 1030–1041

Bacher C, Gangnery A, Cugier P, Mongruel R, Strand O, Frangoudes K (2019) Spatial, ecological and social dimensions of assessments for bivalve farming management. In: Smaal A, Ferreira J, Grant J, Petersen J, Strand Ø (eds) Goods and services of marine bivalves. Springer, Cham, p 527–549

Bayne BL (2017) Biology of oysters. Developments in Aquaculture and Fisheries Science, Vol 41. Academic Press, London

Bec B, Husseini-Ratrema J, Collos Y, Souchu P, Vaquer A (2005) Phytoplankton seasonal dynamics in a Mediterranean coastal lagoon: emphasis on the picoeukaryote community. J Plankton Res 27:881–894

Bernard JP, Frenod E, Rousseau A (2013) Modeling confinement in Etang de Thau: numerical simulations and multiscale aspects. Dyn Syst Differ Equations (DCDS Suppl)2013:69–76

Booth DJ, Brosnan DM (1995) The role of recruitment dynamics in rocky shore and coral reef fish communities. Adv Ecol Res 26:309–385

Brenner M, Fraser D, Van Nieuwenhove K, O'Beirn F and others (2014) Bivalve aquaculture transfers in Atlantic Europe. B. Environmental impacts of transfer activities. Ocean Coast Manage 89:139–146

Bryan-Brown DN, Brown CJ, Hughes JM, Connolly RM (2017) Patterns and trends in marine population connectivity research. Mar Ecol Prog Ser 585:243–256

Carnegie RB, Arzul I, Bushek D (2016) Managing marine mollusc diseases in the context of regional and international commerce: policy issues and emerging concerns. Philos Trans R Soc B 371:20150215

Collos Y, Bec B, Jauzein C, Abadie E and others (2009) Oligotrophication and emergence of picocyanobacteria and a toxic dinoflagellate in Thau lagoon, southern France. J Sea Res 61:68–75

Coon SL, Fitt WK, Bonar DB (1990) Competence and delay of metamorphosis in the Pacific oyster *Crassostrea gigas.* Mar Biol 106:379–387

Cowen RK, Sponaugle S (2009) Larval dispersal and marine population connectivity. Annu Rev Mar Sci 1:443–466

Cowen RK, Gawarkiewicz G, Pineda J, Thorrold SR, Werner FE (2007) Population connectivity in marine systems. Oceanography (Wash DC) 20:14–21

Dame RF, Prins TC (1998) Bivalve carrying capacity in coastal ecosystems. Aquat Ecol 31:409–421

Deslous-Paoli JM, Mazouni N, Souchu P, Landrein S, Pichot P, Juge C (1993) Oyster farming impact on the environment of a Mediterranean lagoon (THAU). In: Dame RF (ed) Bivalve filter feeders in estuarine and coastal ecosystem processes. Springer, Berlin, p 519–521

Dupuy C, Vaquer A, Lam-Höai T, Rougier C and others (2000) Feeding rate of the oyster *Crassostrea gigas* in a natural planktonic community of the Mediterranean Thau lagoon. Mar Ecol Prog Ser 205:171–184

Elsäßer B, Fariñas-Franco JM, Wilson CD, Kregting L, Roberts D (2013) Identifying optimal sites for natural recovery and restoration of impacted biogenic habitats in a special area of conservation using hydrodynamic and habitat suitability modelling. J Sea Res 77:11–21

Fiandrino A, Ouisse V, Dumas F, Lagarde F and others (2017) Spatial patterns in coastal lagoons related to the hydrodynamics of seawater intrusion. Mar Pollut Bull 119:132–144

Filgueira R, Guyondet T, Comeau LA, Grant J (2014) A fully-spatial ecosystem-DEB model of oyster (*Crassostrea virginica*) carrying capacity in the Richibucto Estuary, eastern Canada. J Mar Syst 136:42–54

Filgueira R, Guyondet T, Bacher C, Comeau LA (2015) Informing marine spatial planning (MSP) with numerical modelling: a case-study on shellfish aquaculture in Malpeque Bay (eastern Canada). Mar Pollut Bull 100: 200–216

Fitt WK, Coon SL, Walch M, Weiner RM, Colwell RR, Bonar DB (1990) Settlement behavior and metamorphosis of

oyster larvae (*Crassostrea gigas*) in response to bacterial supernatants. Mar Biol 106:389–394

Gaines S, Brown S, Roughgarden J (1985) Spatial variation in larval concentrations as a cause of spatial variation in settlement for the barnacle, *Balanus glandula.* Oecologia 67:267–272

Gangnery A, Bacher C, Buestel D (2004) Modelling oyster population dynamics in a Mediterranean coastal lagoon (Thau, France): sensitivity of marketable production to environmental conditions. Aquaculture 230:323–347

Ghezzo M, De Pascalis F, Umgiesser G, Zemlys P, Sigovini M, Marcos C, Pérez-Ruzafa A (2015) Connectivity in three European coastal lagoons. Estuaries Coasts 38: 1764–1781

Griffith DM, Veech JA, Marsh CJ (2016) cooccur: probabilistic species co-occurrence analysis in R. J Stat Softw 69: 1–17

Guelorget O, Perthuisot JP (1992) Paralic ecosystems. Biological organization and functioning. Vie Milieu 42: 215–251

Guelorget O, Perthuisot J, Frisoni GF, Monti D (1987) Le rôle du confinement dans l'organisation biogéologique de la lagune de Nador (Maroc). Oceanol Acta 10:435–444

Holgate SJ, Matthews A, Woodworth PL, Rickards LJ and others (2013) New data systems and products at the permanent service for mean sea level. J Coast Res 288: 493–504

Hori M, Hamaoka H, Hirota M, Lagarde F and others (2018) Application of the coastal ecosystem complex concept toward integrated management for sustainable coastal fisheries under oligotrophication. Fish Sci 84:283–292

Hunt HL, Scheibling RE (1997a) Role of early post-settlement mortality in recruitment of benthic marine invertebrates. Mar Ecol Prog Ser 155:269–301

Hunt HL, Scheibling RE (1997b) Recruitment of benthic marine invertebrates. Mar Ecol Prog Ser 155:269–301

ICES (2011) Report of the Working Group on Marine Shellfish Culture (WGMASC), 5–8 April 2011, La Trinité-sur-Mer, France. ICES CM 2011/SSGHIE:08

Jarry V, Fiala M, Frisoni GF, Jacques G, Neveux J, Panouse M (1990) The spatial distribution of phytoplankton in a Mediterranean lagoon (Etang de Thau). Oceanol Acta 13:503–512

Keough MJ, Downes BJ (1982) Recruitment of marine invertebrates: the role of active larval choices and early mortality. Oecologia 54:348–352

Kjerfve B (1994) Coastal lagoons. In: Kjerfve B (ed) Coastal lagoon processes. Elsevier Oceanography Series No. 60. Elsevier, Amsterdam, p 1–8

Lagarde F, Fiandrino A, Richard M, Bernard I and others (2015) Déterminisme du recrutement larvaire de l'huître creuse (*Crassostrea gigas*) dans la lagune de Thau. http://archimer.ifremer.fr/doc/00279/39054/

Lagarde F, Roque d'Orbcastel E, Ubertini M, Mortreux S and others (2017) Recruitment of the Pacific oyster *Crassostrea gigas* in a shellfish-exploited Mediterranean lagoon: discovery, driving factors and a favorable environmental window. Mar Ecol Prog Ser 578:1–17

Lagarde F, Richard M, Bec B, Roques C and others (2018) Trophic environments influence size at metamorphosis and recruitment performance of the Pacific oyster. Mar Ecol Prog Ser 602:135–153

Lagarde F, Ubertini M, Mortreux S, Perignon A and others (2019) Heterogeneity of Japanese oyster (*Crassostrea gigas*) spat collection in a shellfish farmed Mediterranean lagoon. In: Komatsu T, Ceccaldi HJ, Yoshida J, Prouzet P, Henocque Y (eds) Oceanography challenges to future earth: human and natural impacts on our seas. Springer Nature, Cham, p 341–350

Lam-Hoai T, Rougier C, Lasserre G (1997) Tintinnids and rotifers in a northern Mediterranean coastal lagoon. Structural diversity and function through biomass estimations. Mar Ecol Prog Ser 152:13–25

Lazure P, Dumas F (2008) An external–internal mode coupling for a 3D hydrodynamical model for applications at regional scale (MARS). Adv Water Resour 31:233–250

LeCorre N (2013) Variabilité de la connectivité et du recrutement au sein d'une métapopulation marine. PhD thesis, Laval University, Québec City

Lefebvre S, Barillé L, Clerc M (2000) Pacific oyster *Crassostrea gigas* feeding responses to a fish-farm effluent. Aquaculture 187:185–198

Lehane C, Davenport J (2004) Ingestion of bivalve larvae by *Mytilus edulis*: experimental and field demonstrations of larviphagy in farmed blue mussels. Mar Biol 145: 101–107

Levin LA (2006) Recent progress in understanding larval dispersal: new directions and digressions. Integr Comp Biol 46:282–297

Olson RR, Olson MH (1989) Food limitation of planktotrophic marine invertebrate larvae: Does it control recruitment success? Annu Rev Ecol Syst 20:225–247

Pawlik JR (1992) Chemical ecology of the settlement of benthic marine marine invertebrates. Oceanogr Mar Biol Annu Rev 30:273–335

Pechenik JA (2006) Larval experience and latent effects—metamorphosis is not a new beginning. Integr Comp Biol 46:323–333

Pérez-Ruzafa A, De Pascalis F, Ghezzo M, Quispe-Becerra JI and others (2019) Connectivity between coastal lagoons and sea: asymmetrical effects on assemblages' and population's structure. Estuar Coast Shelf Sci 216:171–186

Pernet F, Malet N, Pastoureaud A, Vaquer A, Quéré C, Dubroca L (2012) Marine diatoms sustain growth of bivalves in a Mediterranean lagoon. J Sea Res 68:20–32

Pineda J, Reyns N (2018) Larval transport in the coastal zone: biological and physical processes. In: Carrier T, Reitzel A, Heyland A (eds) Evolutionary ecology of marine invertebrate larvae. Oxford University Press, Oxford, p 145–163

Pineda J, Hare JA, Sponaugle S (2007) Larval transport and dispersal in the coastal ocean and consequences for population connectivity. Oceanography (Wash DC) 20:22–39

Pineda J, Reyns NB, Starczak VR (2009) Complexity and simplification in understanding recruitment in benthic populations. Popul Ecol 51:17–32

Plus M, La Jeunesse I, Bouraoui F, Zaldívar JM, Chapelle A, Lazure P (2006) Modelling water discharges and nitrogen inputs into a Mediterranean lagoon: impact on the primary production. Ecol Modell 193:69–89

Pouvreau S (2016) Observer, Analyser et Gérer la variabilité de la reproduction et du recrutement de l'huître creuse en France: Le Réseau Velyger. Rapport annuel 2015. R.INT.BREST RBE/PFOM/PI 2016-1. http://archimer.ifremer.fr/doc/00334/44533/

Pouvreau S, Bellec G, Le Souchu P, Queau I and others (2013) Observer, Analyser et Gérer la variabilité de la reproduction et du recrutement de l'huître creuse en France: Le Réseau Velyger. Rapport annuel 2012. http://doi.org/10.13155/31091

Pouvreau S, Petton S, Queau I, Haurie A and others (2015) Observer, Analyser et Gérer la variabilité de la reproduction et du recrutement de l'huître creuse en France: Le Réseau Velyger. Rapport annuel 2014. https://wwz.ifremer.fr/velyger/Rapports-Annuels/Annee-2014

Pouvreau S, Maurer D, Auby I, Lagarde F and others (2016) VELYGER database: the oyster larvae monitoring French project. http://doi.org/10.17882/41888

Pouvreau S, Fleury E, Petton S, Le Roy V and others (2018) Observer, Analyser et Gérer la variabilité de la reproduction et du recrutement de l'huître creuse en France: Le Réseau Velyger. Rapport annuel 2017. https://wwz.ifremer.fr/velyger/Rapports-Annuels/Annee-2017

R Core Team (2015) R: a language and environment for statistical computing. R Foundation for Statistical Computing, Vienna

Rayssac N, Pérignon A, Gervasoni E, Pernet F, LeGall P, Lagarde F (2012) Evaluation du potentiel d'approvisionnement naturel en naissains d'huîtres creuses en Méditerranée - Rapport Final - Projet PRONAMED 2010-2011. Comité Régional de Conchyliculture de Méditerranée, Mèze

REPHY (French Observation and Monitoring program for Phytoplankton and Hydrology) (2017) REPHY dataset—French observation and monitoring program for phytoplankton and hydrology in coastal waters. 1987-2016 Metropolitan data. SEANOE. http://doi.org/10.17882/47248

Rodríguez SR, Ojeda FP, Inestrosa NC (1993) Settlement of benthic marine invertebrates. Mar Ecol Prog Ser 97: 193–207

Rose M (1933) Copépodes pélagiques. Faune de France, Vol 26. Paul Lechevalier, Paris

Roughgarden J, Gaines SD, Possingham H (1988) Recruitment dynamics in complex life cycles. Science 241: 1461–1466

Smyth D, Kregting L, Elsäßer B, Kennedy R, Roberts D (2016) Using particle dispersal models to assist in the conservation and recovery of the overexploited native oyster (*Ostrea edulis*) in an enclosed sea lough. J Sea Res 108:50–59

Solidoro C, Melaku Canu D, Cucco A, Umgiesser G (2004) A partition of the Venice Lagoon based on physical properties and analysis of general circulation. J Mar Syst 51:147–160

Souchu P, Vaquer A, Collos Y, Landrein S, Deslous-Paoli JM, Bibent B (2001) Influence of shellfish farming activities on the biogeochemical composition of the water column in Thau lagoon. Mar Ecol Prog Ser 218: 141–152

Souchu P, Bec B, Smith VH, Laugier T and others (2010) Patterns in nutrient limitation and chlorophyll *a* along an anthropogenic eutrophication gradient in French Mediterranean coastal lagoons. Can J Fish Aquat Sci 67: 743–753

Thomas Y, Dumas F, Andréfouët S (2016) Larval connectivity of pearl oyster through biophysical modelling; evidence of food limitation and broodstock effect. Estuar Coast Shelf Sci 182:283–293

Todd CD (1998) Larval supply and recruitment of benthic invertebrates: Do larvae always disperse as much as we believe? Hydrobiologia 375/376:1–21

Toupoint N, Gilmore-Solomon L, Bourque F, Myrand B, Pernet F, Olivier F, Tremblay R (2012) Match/mismatch between the *Mytilus edulis* larval supply and seston quality: effect on recruitment. Ecology 93:1922–1934

Troost K, Kamermans P, Wolff WJ (2008a) Larviphagy in native bivalves and an introduced oyster. J Sea Res 60: 157–163

Troost K, Veldhuizen R, Stamhuis EJ, Wolff WJ (2008b) Can bivalve veligers escape feeding currents of adult bivalves? J Exp Mar Biol Ecol 358:185–196

Vaquer A, Troussellier M, Courties C, Bibent B (1996) Standing stock and dynamics of picophytoplankton in the Thau Lagoon (northwest Mediterranean coast). Limnol Oceanogr 41:1821–1828

Veech JA (2013) A probabilistic model for analysing species co-occurrence. Glob Ecol Biogeogr 22:252–260

Wing SR, Botsford LW, Morgan LE, Diehl JM, Lundquist CJ (2003) Inter-annual variability in larval supply to populations of three invertebrate taxa in the northern California Current. Estuar Coast Shelf Sci 57:859–872

Editorial responsibility: Inna Sokolova, Rostock, Germany

Submitted: October 2, 2018; Accepted: September 30, 2019
Proofs received from author(s): December 2, 2019